NAVAL POSTGRADUATE SCHOOL

MONTEREY, CALIFORNIA

THESIS

REDUCING ELECTROMAGNETIC INTERFERENCE IN A GRID TIED SINGLE PHASE POWER INVERTER

by

Jason Hassan Valiani

September 2016

Thesis Advisor: Giovanna Oriti
Thesis Co-Advisor: Alexander Julian

Approved for public release. Distribution is unlimited.

THIS PAGE INTENTIONALLY LEFT BLANK

REPORT DOCUMENTATION PAGE		*Form Approved OMB No. 0704–0188*
Public reporting burden for this collection of information is estimated to average 1 hour per response, including the time for reviewing instruction, searching existing data sources, gathering and maintaining the data needed, and completing and reviewing the collection of information. Send comments regarding this burden estimate or any other aspect of this collection of information, including suggestions for reducing this burden, to Washington headquarters Services, Directorate for Information Operations and Reports, 1215 Jefferson Davis Highway, Suite 1204, Arlington, VA 22202-4302, and to the Office of Management and Budget, Paperwork Reduction Project (0704-0188) Washington, DC 20503.		
1. AGENCY USE ONLY (*Leave blank*)	**2. REPORT DATE** September 2016	**3. REPORT TYPE AND DATES COVERED** Master's thesis
4. TITLE AND SUBTITLE REDUCING ELECTROMAGNETIC INTERFERENCE IN A GRID TIED SINGLE PHASE POWER INVERTER		**5. FUNDING NUMBERS**
6. AUTHOR(S) Jason Hassan Valiani		
7. PERFORMING ORGANIZATION NAME(S) AND ADDRESS(ES) Naval Postgraduate School Monterey, CA 93943-5000		**8. PERFORMING ORGANIZATION REPORT NUMBER**
9. SPONSORING /MONITORING AGENCY NAME(S) AND ADDRESS(ES) N/A		**10. SPONSORING / MONITORING AGENCY REPORT NUMBER**
11. SUPPLEMENTARY NOTES The views expressed in this thesis are those of the author and do not reflect the official policy or position of the Department of Defense or the U.S. Government. IRB Protocol number ____N/A____.		
12a. DISTRIBUTION / AVAILABILITY STATEMENT Approved for public release. Distribution is unlimited.		**12b. DISTRIBUTION CODE**

13. ABSTRACT (maximum 200 words)

As the demand for a more robust and reliable electrical grid continues to grow, the United States Navy is determined to find effective energy solutions. The use of energy management systems (EMS) and uninterruptible power systems (UPS) can be seen both ashore and afloat. Most UPS and EMS are comprised of power inverters. These inverters must comply with the military standards for conducted emissions. In this thesis, two different modulation strategies, bipolar and unipolar, are explored. The primary goal is to understand the effects each modulation strategy has on the conducted electromagnetic interference (EMI) and then try to eliminate that EMI in the common and differential mode paths.

In order to accomplish this, a laboratory experiment on an EMS using both modulation strategies was performed. The EMS was in grid-connected mode. Once the differential and common mode currents and voltages were obtained, Simulink was used to model the laboratory EMS. Once there was confidence in the model's ability to predict the laboratory behavior, a line impedance stabilization network (LISN) was added to the design. Comparing the LISN voltage to the MIL-STD showed that the current model was not within limits. The addition of a passive filter proved to minimize the conducted EMI for a single-phase grid-tied inverter.

14. SUBJECT TERMS single-phase inverter, conducted emissions			**15. NUMBER OF PAGES** 61
			16. PRICE CODE
17. SECURITY CLASSIFICATION OF REPORT Unclassified	**18. SECURITY CLASSIFICATION OF THIS PAGE** Unclassified	**19. SECURITY CLASSIFICATION OF ABSTRACT** Unclassified	**20. LIMITATION OF ABSTRACT** UU

NSN 7540–01-280-5500

Standard Form 298 (Rev. 2–89)
Prescribed by ANSI Std. 239–18

THIS PAGE INTENTIONALLY LEFT BLANK

**REDUCING ELECTROMAGNETIC INTERFERENCE IN A GRID TIED
SINGLE PHASE POWER INVERTER**

Jason Hassan Valiani
Lieutenant, United States Navy
B.S., United States Naval Academy, 2010

Submitted in partial fulfillment of the
requirements for the degree of

MASTER OF SCIENCE IN ELECTRICAL ENGINEERING

from the

**NAVAL POSTGRADUATE SCHOOL
September 2016**

Approved by: Giovanna Oriti
Thesis Advisor

Alexander Julian
Co-Advisor

R. Clark Robertson
Chair, Department of Electrical and Computer Engineering

THIS PAGE INTENTIONALLY LEFT BLANK

ABSTRACT

As the demand for a more robust and reliable electrical grid continues to grow, the United States Navy is determined to find effective energy solutions. The use of energy management systems (EMS) and uninterruptible power systems (UPS) can be seen both ashore and afloat. Most UPS and EMS are comprised of power inverters. These inverters must comply with the military standards for conducted emissions. In this thesis, two different modulation strategies, bipolar and unipolar, are explored. The primary goal is to understand the effects each modulation strategy has on the conducted electromagnetic interference (EMI) and then try to eliminate that EMI in the common and differential mode paths.

In order to accomplish this, a laboratory experiment on an EMS using both modulation strategies was performed. The EMS was in grid-connected mode. Once the differential and common mode currents and voltages were obtained, Simulink was used to model the laboratory EMS. Once there was confidence in the model's ability to predict the laboratory behavior, a line impedance stabilization network (LISN) was added to the design. Comparing the LISN voltage to the MIL-STD showed that the current model was not within limits. The addition of a passive filter proved to minimize the conducted EMI for a single-phase grid-tied inverter.

THIS PAGE INTENTIONALLY LEFT BLANK

TABLE OF CONTENTS

THIS PAGE INTENTIONALLY LEFT BLANK

LIST OF FIGURES

LIST OF TABLES

THIS PAGE INTENTIONALLY LEFT BLANK

LIST OF ACRONYMS AND ABBREVIATIONS

AC	alternating current
CM	common mode
CCM	continuous conduction mode
DC	direct current
DC/AC	direct current to alternating current
DCM	discontinuous conduction mode
DM	differential mode
EMI	electromagnetic interference
EUT	equipment under test
EMS	energy management system
FFT	fast Fourier transform
FPGA	field programmable gate array
IGBT	insulated-gate bipolar transistor
LISN	line impedance stabilization network
PWM	pulse width modulation
RMS	root mean squared
UPS	uninterruptible power system

THIS PAGE INTENTIONALLY LEFT BLANK

ACKNOWLEDGMENTS

I would like to take the opportunity to thank my thesis advisors, Professor Oriti and Professor Julian, for guiding me during my tenure at NPS. In addition, I would also like to thank my wife, Emalena, who has continually encouraged me throughout this process.

THIS PAGE INTENTIONALLY LEFT BLANK

I.   INTRODUCTION

In the ever-changing landscape of energy, the United States Navy understands the importance of energy security both ashore and afloat [1]. One of the keys to energy independence is having a reliable electrical grid that is not dependent on the commercial grid. Furthermore, it cannot be susceptible to natural disasters or vulnerable to cyber-attacks, as these are critical times in which the Navy has to be operational [1].

With the growing demand for a reliable electrical grid, backup power supplies and energy management systems are a necessity. Systems such as server racks, gyros and many other vital pieces of equipment require an uninterruptible power system (UPS) in the event of fault or failure on the grid while at sea. Energy management systems (EMS) used at shore facilities allow for potential faults in the commercial grid while providing a backup source of power to critical infrastructure. Redundant power systems both ashore and afloat include direct current-to-alternating current (DC/AC) power converters, also known as inverters.

Power inverters come in many different topologies that depend on the end users' requirements and design parameters. For my research, we explore the H-bridge inverter using insulated-gate bipolar transistors (IGBTs). IGBTs are power semiconductors used as switches inside the inverter and controlled via pulse-width modulation (PWM).

There are various PWM strategies, and each has particular benefits and shortcomings. This research focuses on both unipolar and bipolar PWM. Each one of these methods affects the system differently. In order to understand the effects of these modulation strategies, we explore the common mode (CM) and differential mode (DM) currents and voltages of the system. Using this analysis, we can then design a filter that will aid in the reduction of conducted electromagnetic interference (EMI).

Conducted EMI is a common problem in power inverters due to high switching frequencies, causing the IGBTs to rapidly turn on or turn off. The result of this high frequency switching causes high voltage and current changes with respect to time [2]. These changes can be seen both in the differential and common modes. For the purposes

of this thesis, we look to reduce the conducted EMI to ensure grid stability. Military standard MIL-STD 461-E [3] is the design metric used.

The goal of this research is to minimize the conducted EMI for a single-phase grid tied power inverter using the best combination of passive filters and PWM strategy. Comparing the CM and DM conducted emissions along with different PWM methods and passive filters allows us to determine the best method to minimize the overall size of the single-phase inverter. Below is a brief outline used to accomplish this goal.

- Design a Simulink model for a single-phase power inverter, to include both unipolar and bipolar PWM. The model features CM as well as DM paths.

- Verify that the Simulink model is accurate by setting up a laboratory prototype and comparing the simulated waveforms to the experimental measurements. Then, refine the computer model to reflect the experimental data more accurately.

- Experimentally validate the model and design the appropriate filters for both bipolar and unipolar PWM to help reduce the conducted EMI.

- Compare the results of each PWM strategy against MIL-STD 461 and discuss the pros and cons of each design.

II.   BACKGROUND INFORMATION

Power inverters are very common in the United States Navy's power systems. With a wide range of uses, from backup power supplies to electric drives, they are in just about every space onboard a warship. Their size can range from very small to very large based on the desired application. In its simplest form, a power inverter converts DC into AC. The use of an H-bridge inverter, as shown in Figure 1, along with PWM creates an output voltage that is a 60-Hz sine wave.

The basic inverter model shown in Figure 1 consists of four main parts: the H-bridge, PWM generator, source and load. In some instances, a boost converter is required between the DC source and the H-bridge depending on the desired input voltage. Adding a boost converter to the circuit may add unwanted harmonics, which can be resolved with the addition of a filter.
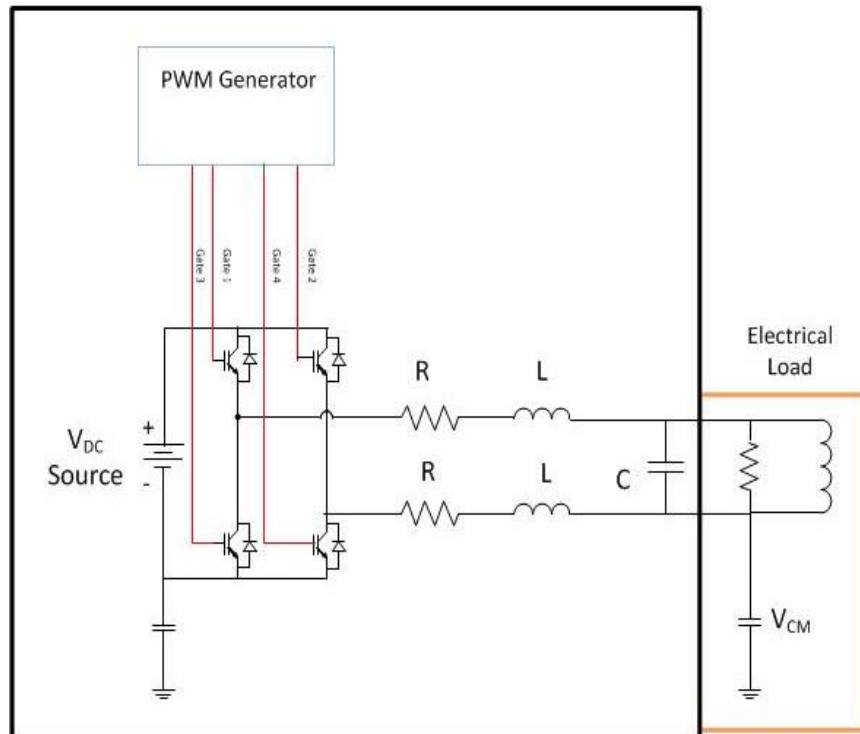

Figure 1.   Basic Model of DC-to-AC Inverter.

A.   BOOST CONVERTER

A boost converter, as seen in Figure 2, steps up the source voltage V_{DC} to a desired output voltage V_{OUT} by varying the duty cycle D. In general, there are three modes of operation for a boost converter: continuous-conduction mode (CCM), barely CCM, and discontinuous-conduction mode (DCM) [4]. The relationship between input and output voltage with respect to the duty cycle in CCM can be described as $V_{out} = V_{DC}/(1-D)$. For the purposes of this thesis, we assume the CCM operates with an approximate duty cycle D of 50%.
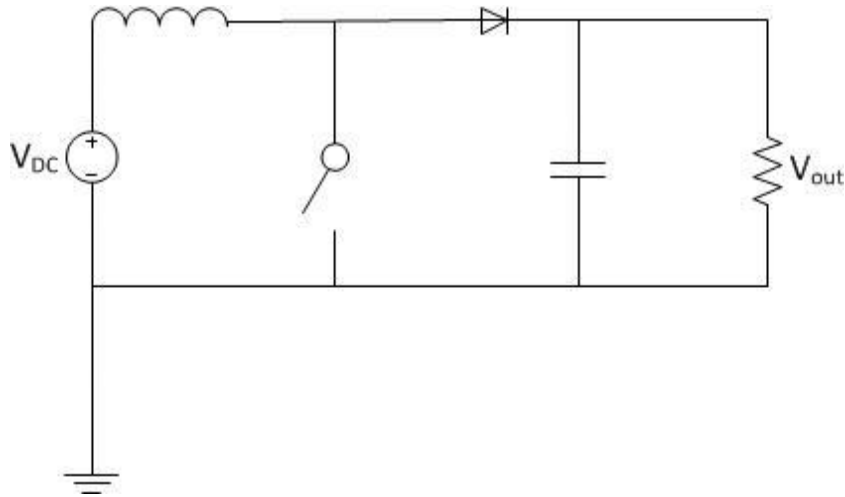
Figure 2.   Electrical Schematic of a Boost Converter.

B.   PULSE-WIDTH MODULATION

An IGBT-based H-bridge inverter controlled with pulse-width modulation transforms a DC source voltage into an AC sine wave. Sending gating signals to the H-bridge at a predetermined frequency turns the IGBTs on and off. Several PWM techniques exist in which to accomplish this. When deciding on which technique to use, consider the following: the technique must have good utilization of the DC source, low switching losses and low output voltage amplitudes for the lower order harmonics [5]. Taking the aforementioned into consideration, we consider both unipolar and bipolar PWM.

1. Bipolar Voltage Switching

Bipolar PWM compares a sine wave $v_{control}$ and a triangular wave v_{tri} to gate the IGBTs, as depicted in Figure 3. For this modulation strategy, opposite diagonal switches, gates 1 and 4 and gates 2 and 3 (as shown in Figure 1), are turned on and off in pairs so that the bottom switch receives a gate signal that is the negative of that received by the top switch [4]. This PWM method results in zero CM voltage and current but has a much higher DM voltage and current when compared to unipolar PWM. The logic operation for bipolar PWM is shown in Table 1. Shown in Figure 4 and Figure 5 are the spectral analyses of the DM voltage for both bipolar and unipolar PWM, respectively. For these simulations, the switching frequency was 17.5 kHz. From this, we note that there is more DM voltage in bipolar PWM. The harmonics observed at 17.5 kHz in Figure 4 represent the switching frequency for bipolar PWM.

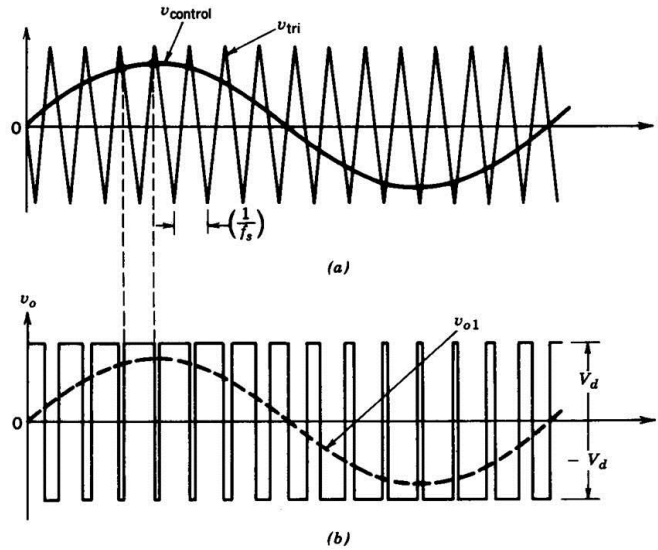Figure 3.   Voltage Wave Forms with Bipolar PWM. Source: [3].

Table 1.   Logic Table for Bipolar PWM. Adapted from [3].

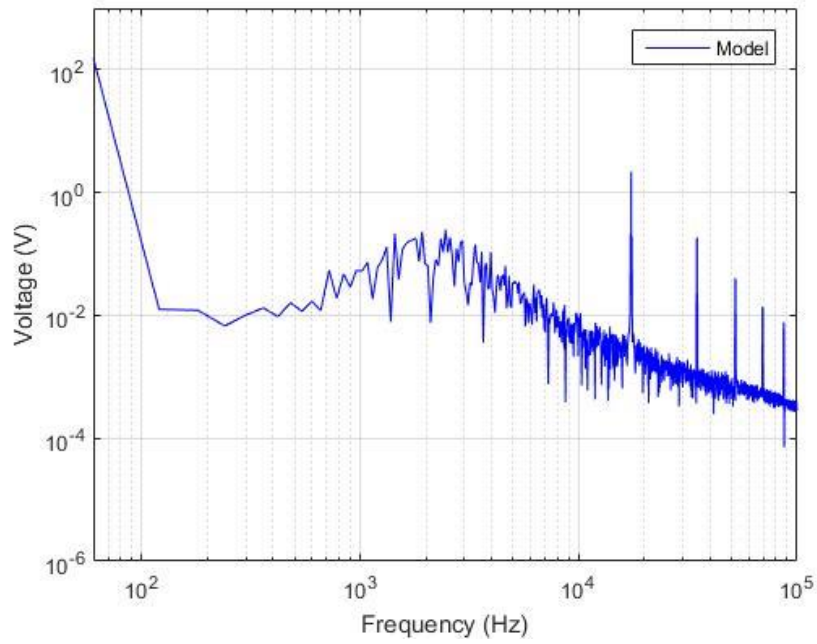| $v_{control} > v_{triangle}$	Gate 1 and 4 On, Gate 2 and 3 Off
$v_{control} < v_{triangle}$	Gate 2 and 3 On, Gate 1 and 4 Off

Figure 4.   Spectral Analysis of DM Voltage for Bipolar PWM.
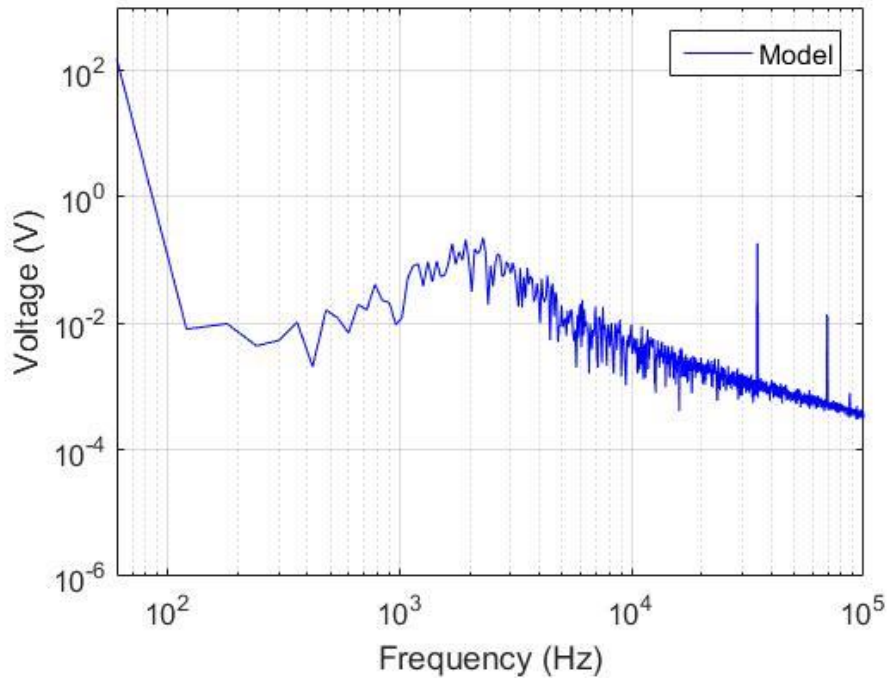

Figure 5.   Spectral Analysis of DM Voltage for Unipolar PWM.

2. Unipolar Voltage Switching

Unipolar PWM controls the top and bottom legs of the inverter separately; in order to do this, the triangular waveform v_{tri} is compared to two sine waves that are 180 degrees out of phase [4]. The logic table provided in Table 2 shows how the reference voltage $v_{control}$ is compared to v_{tri} to produce the gating signals for each IGBT. The resulting voltage waveforms are shown in Figure 6. This method of PWM creates a common mode voltage and current causing conducted EMI; however, less DM EMI is created as compared to bipolar PWM, as shown in Figure 4 and Figure 5. Unipolar PWM has the same switching frequency as bipolar PWM; however, the harmonic analysis shown in Figure 5 indicates that the switching frequency harmonics are suppressed. The first significant harmonics can be found at twice the switching frequency.
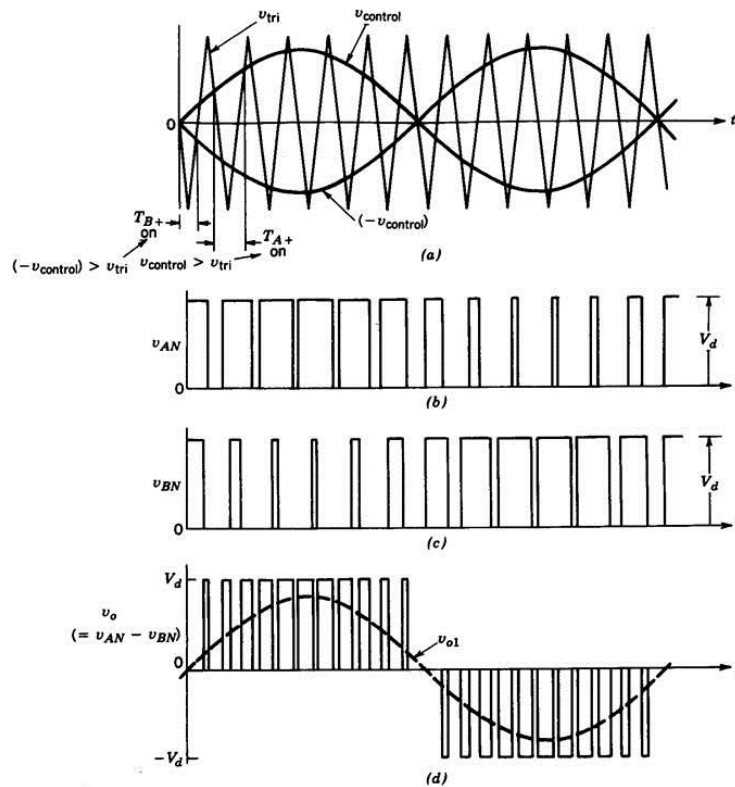

Figure 6.   Voltage Wave Forms for Unipolar PWM. Source: [3].

7

Table 2.　　Logic Table for Unipolar PWM. Adapted from [3].

$v_{control} > v_{triangle}$	Gate 1 on and $v_{AN} = V_d$
$v_{control} < v_{triangle}$	Gate 2 on and $v_{AN} = 0$
$-v_{control} > v_{triangle}$	Gate 3 on and $v_{BN} = V_d$
$-v_{control} < v_{triangle}$	Gate 4 on and $v_{BN} = 0$

C.　　COMMON MODE PATH

Using unipolar or bipolar PWM creates conducted emmisions. Common mode currents flow through parasitic capacitive coupling to ground while DM currents flow to and from their source. Understanding how these currents flow is a key aspect in understanding how to ultimately reduce both CM and DM emmisions. The CM path is shown in Figure 7. Using Kirchoff's voltage law, we obtain

$$V_a - L\frac{di_a}{dt} - Ri_a - V_{ground} = 0 \; , \tag{1}$$

$$V_b - L\frac{di_b}{dt} - Ri_b - V_{ground} = 0 \; . \tag{2}$$

Equations (1) and (2) represent the voltage loops in the top and bottom leg of the inverter. Setting (1) equal to (2), we get (3)

$$V_a + V_b - L\frac{di}{dt}(i_a + i_b) - R(i_a + i_b) = 2\,V_{ground} \; . \tag{3}$$

Equation (3) assumes that the voltage in both legs of the inverter are equal to one another. If $i_a = -i_b$, we get (4). Using

$$V_{ground} = \frac{V_A + V_B}{2} \; , \tag{4}$$

we get for bipolar PWM $V_{ground} = 0$ and for unipolar PWM $V_{ground} \neq 0$.
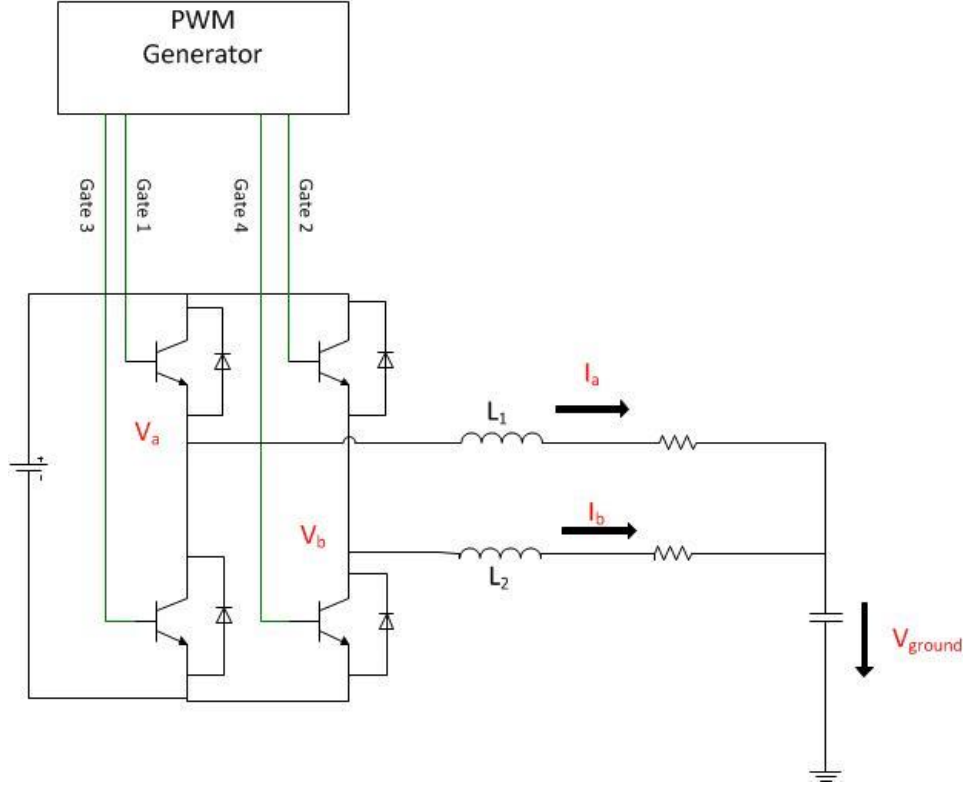
Figure 7.   Common Mode Emissions in a Single-Phase Inverter.

D.   FILTER BASICS

The advancement of power electronics has increased the speed of switching devices and caused filters to become a necessity in energy management systems. For the purposes for this thesis, we explore passive filters to minimize the conducted EMI. In general, a filter's job is to attenuate the harmonics at certain frequencies. The cutoff frequency f_{cutoff} is determined by the size of the inductor L and capacitor C. Using

$$f_{cutoff} = \frac{1}{2\pi\sqrt{LC}}, \tag{5}$$

we can determine the cutoff frequency of a filter and attenuate any unwanted frequencies [6]. In particular, for an H-bridge inverter, the filter must attenuate the switching frequency harmonics. We note from Figure 4 and Figure 5 that unipolar PWM has larger higher-order harmonics as compared to bipolar PWM; therefore, the physical size of the DM filter is smaller when unipolar PWM is used.

9

E. MILITARY STANDARD

Several standards exist in relation to conducted EMI. The U.S. Department of Defense MIL-STD 461 establishes the requirements for the control of electromagnetic interference [3]. The emissions and susceptibility requirements, CE102, are "applicable from 10 kHz to 10 MHz for all power leads, including returns, that obtain power from other sources not part of the equipment under test (EUT)" [3]. The limits for the conducted EMI are shown in Figure 8. In addition to this limit, a 6 dB relaxation is applicable for this thesis because the nominal EUT voltage is 115 V. In order to conduct CE102 measurements, a line impedance stabilization network (LISN) is required. Using a LISN enables us to take voltage readings of the EUT and compare them to the basic curve shown in Figure 8. Using

$$dB\mu V = 20\log_{10}\left(\frac{volts}{1\mu V}\right),\qquad(6)$$

we can convert volts into dBμV [7].

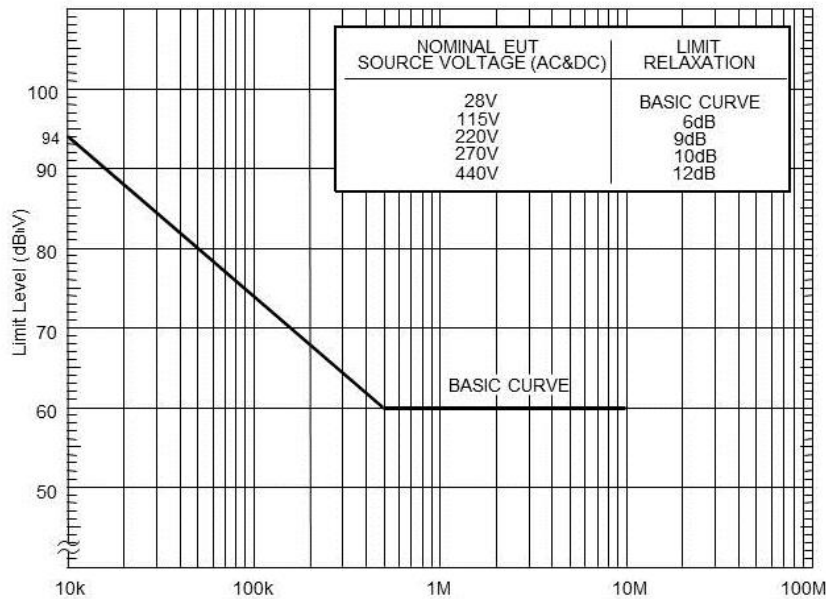| NOMINAL EUT SOURCE VOLTAGE (AC&DC)	LIMIT RELAXATION
28V	BASIC CURVE
115V	6dB
220V	9dB
270V	10dB
440V	12dB

Figure 8.   CE102 Limit (EUT power leads, AC and DC) for All Applications.
Source: [3].

III. VALIDATING THE SIMULINK MODEL

Using a Simulink model to predict the behavior of a single-phase, grid-tied inverter in order to study conducted EMI has advantages and disadvantages. When using a model, one must understand the limitations of the model. For the purpose of this thesis, we use the circuit shown in Figure 9. The currents I_{cm}, I_{ems} and voltage V_{ac} measured in the laboratory prototype are marked on Figure 9. Throughout this chapter, we explain the differences between the laboratory prototype and the Simulink model. The goal of this section is to validate the Simulink model by comparing its simulations to the experimental measurements. If the two match, then the model is considered a valid representation of the laboratory set up.
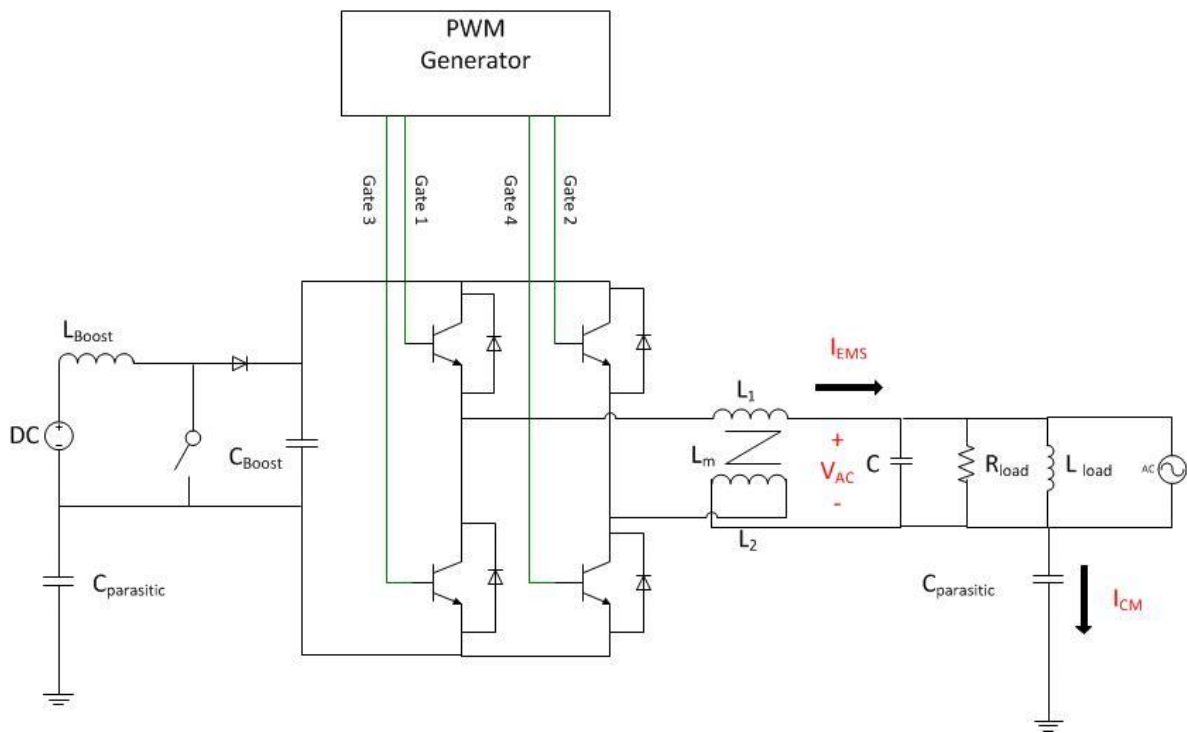

Figure 9.   Circuit Diagram Used to Design Simulink Model.

A.   SIMULINK MODEL DESIGN

The Simulink model shown in Figure 10 replicates the design of the EMS used in the laboratory. The model is comprised of a boost converter, an H-bridge inverter, the duty-cycle generator, the PWM generator, and two LISNs. It is important to note that there are no LISNs in the laboratory experiment. The duty cycle generator, PWM generator, and LISNs are subsystems of the model and are illustrated in Figure 11, Figure 12 and Figure 13, respectively. Elements from the SimPowerSystems library in Simulink were used to create this model.

When designing this single-phase power inverter, the H-bridge switches were modeled as ideal. This allows the delay time in turning the IGBT's on and off to be omitted; this delay is known as blanking time or dead time. Another consideration is how to incorporate the parasitic capacitance inside the circuit in order to model the CM voltage and current. A common practice is to model the parasitic capacitance as a single capacitor to ground at the input and at the output of the system that are represented by C_1 and C_2, respectively [8]. Parasitic capacitance, or stray capacitance, is common in electrical circuits. In general, stray capacitance can come from electronic elements, wires and many other elements inside the circuit. Choosing to model all of the stray capacitance as a single capacitor to ground simplifies the problem vice having to figure out how each component interacts with another. This allows the measurement of the CM current and voltage inside the Simulink model.
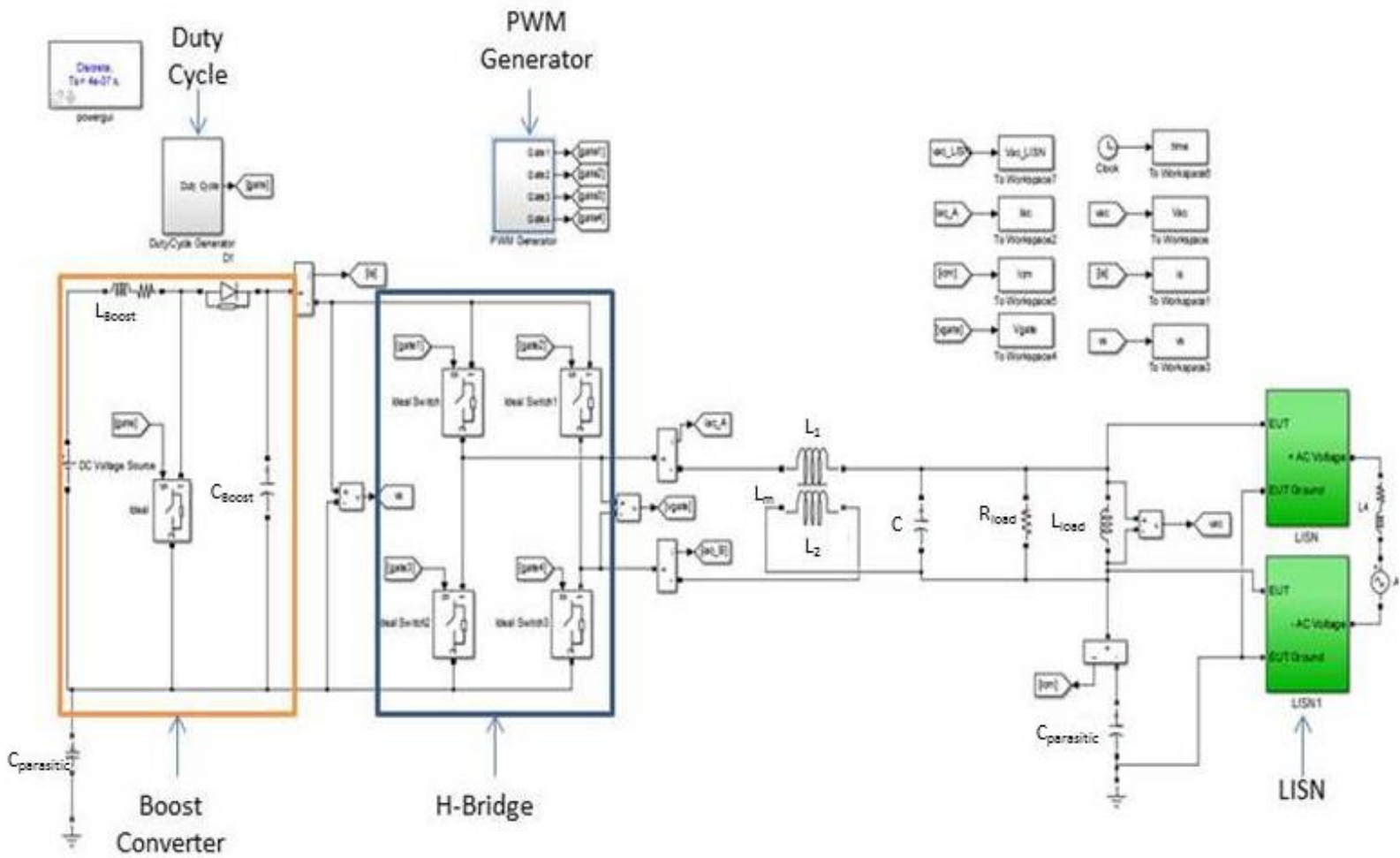
Figure 10.   Simulink Model of Boost Converter with H-bridge Inverter.

13

When designing the PWM generator for the boost converter, initially the duty cycle was 50%, which is normal for a converter operating in CCM. This duty cycle produced too much DC voltage; therefore, the duty cycle was reduced to 47%. Using a constant duty cycle rather than a feedback control system simplifies the model. Using a duty cycle of 47% allows the boost converter to operate in open-loop CCM. This is a practical choice as the load is constant for these simulations. In order to create the subsystem shown in Figure 11, a triangle generator with an amplitude of one, a percent duty value of 0.47 and a relational operator was used. Comparing the constant value of 0.47 to the triangle wave using less than or equal to (<=) logic, we obtain the desired duty cycle. The frequency of the triangle wave is 20 kHz.
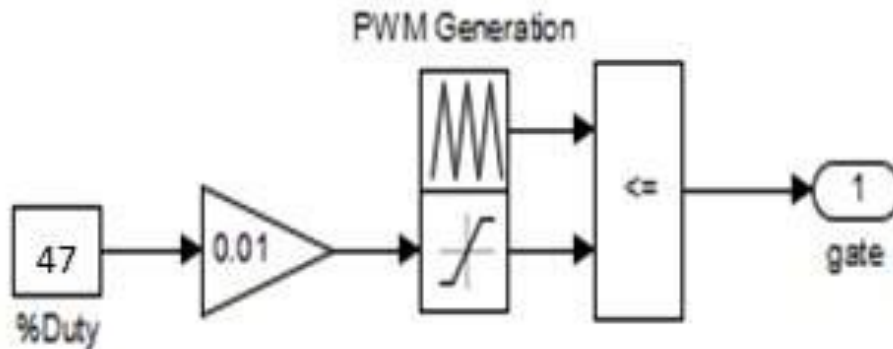

Figure 11.   Simulink Subsystem Model for Duty-Cycle Generator.

The Simulink model shown in Figure 12 represents the design for both unipolar and bipolar PWM. The signals for each gate, both bipolar and unipolar, go to a switch prior to the IGBTs. An input of zero to the switch indicates bipolar PWM, and an input of one indicates unipolar PWM. These models where derived from Tables 1 and 2 in Chapter II. In addition, a control loop was added based on the EMS controller used in the laboratory to keep a constant current of 1.0 A going to the inductor. To accomplish this, a reference current of 1.0 A was used along with the actual DM current. These two currents were then subtracted and a proportional and integral controller was used. The gains of this controller are based on the gains used in the laboratory, K_p= 0.15 and K_I = 6.0.
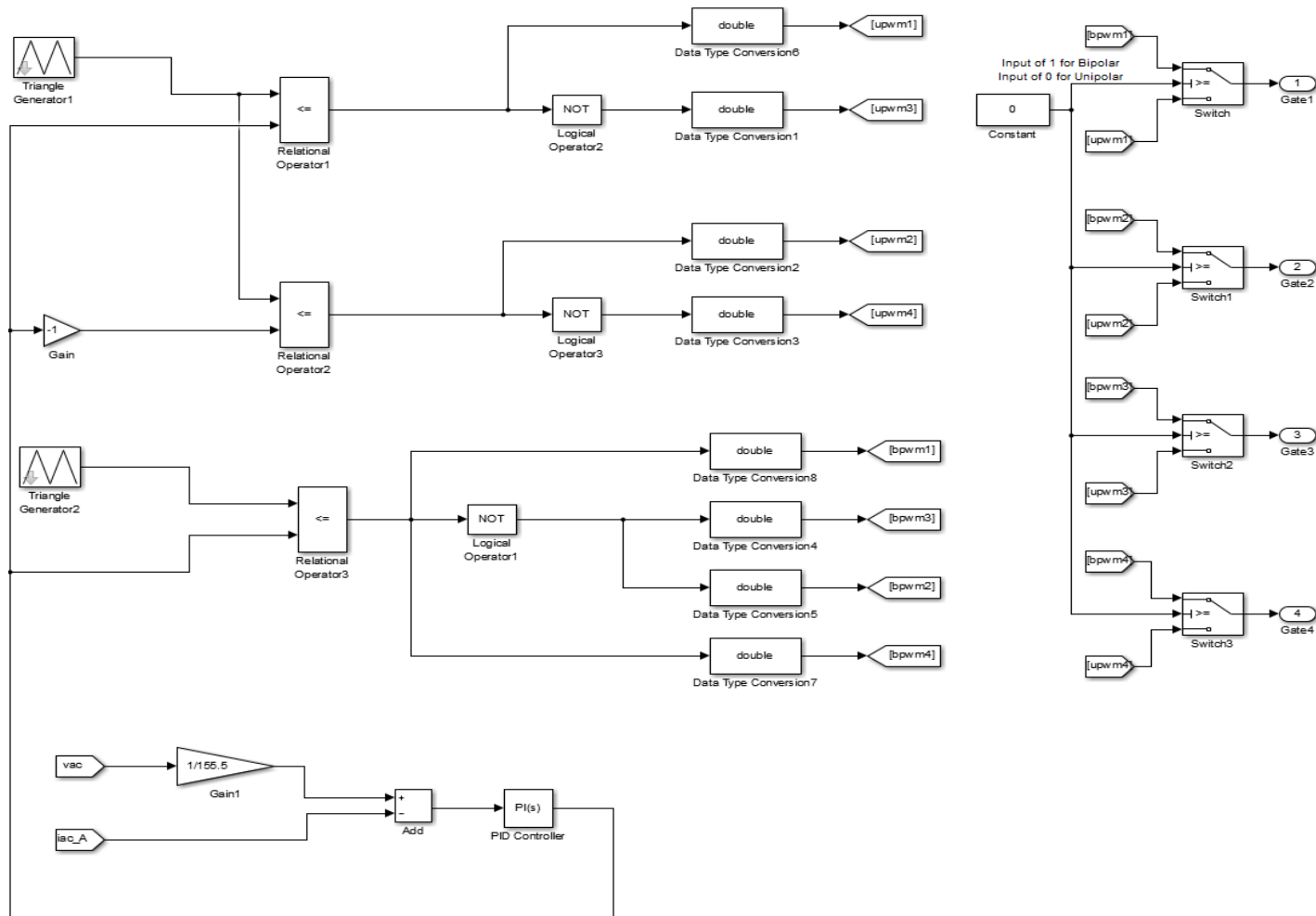
Figure 12.   Simulink Subsystem Model for Unipolar and Bipolar PWM.

15

The final subsystem of the model is the LISN shown in Figure 13. The design for the LISN came from MIL-STD 461 [3]. The measurement setup shown in Figure 14 was used to implement the LISN design in the Simulink model. In general, a LISN can control the power source impedance, which is critical to the test procedure [3]. Using a LISN allows the measurement of the conducted EMI for the equipment under test (EUT).
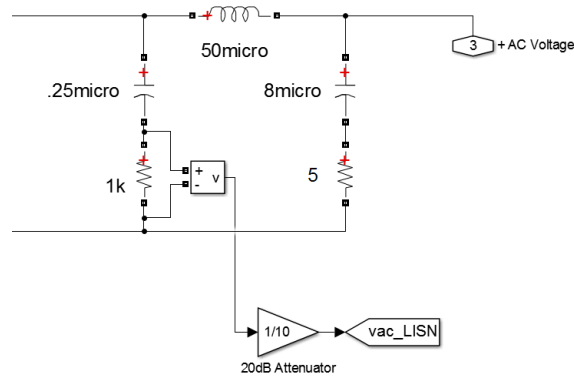

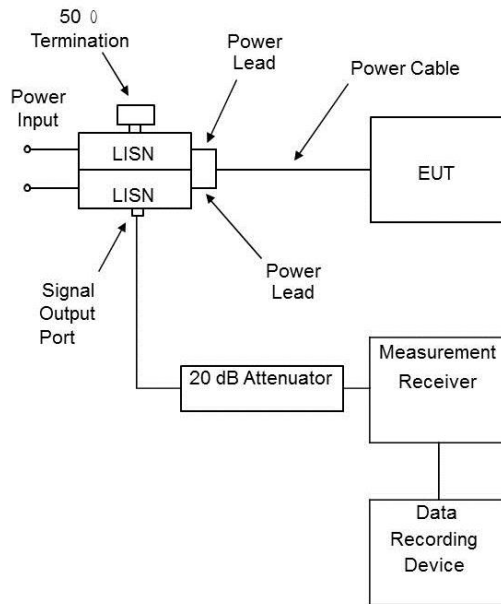Figure 13.   Simulink Subsystem Model of a LISN. Adapted from [3].

Figure 14.   Measurement Setup in Accordance with MIL-STD 46. Source: [3].

16

B.   SIMULINK AND EMS PARAMETERS

The EMS used in the laboratory, shown in Figure 15, includes batteries, a three-leg power module controlled by a field programmable gate array (FPGA), and an output LC filter [9]. The battery pack consists of eight, 12.0-V battery cells connected in series totaling 96.0 V. The battery pack connects to a boost converter and the H-bridge, as shown in Figure 16. The parameters used for the Simulink model and the laboratory experiments are listed in Table 3. The EMS used in the lab has two modes of operation, grid-connected mode and islanding mode. Taking readings while in islanding mode does not fit the criteria of the MIL-STD; therefore, for the purposes of this thesis, the EMS was operated in grid-connected mode. This eliminates the need for the buck converter shown in Figure 16.
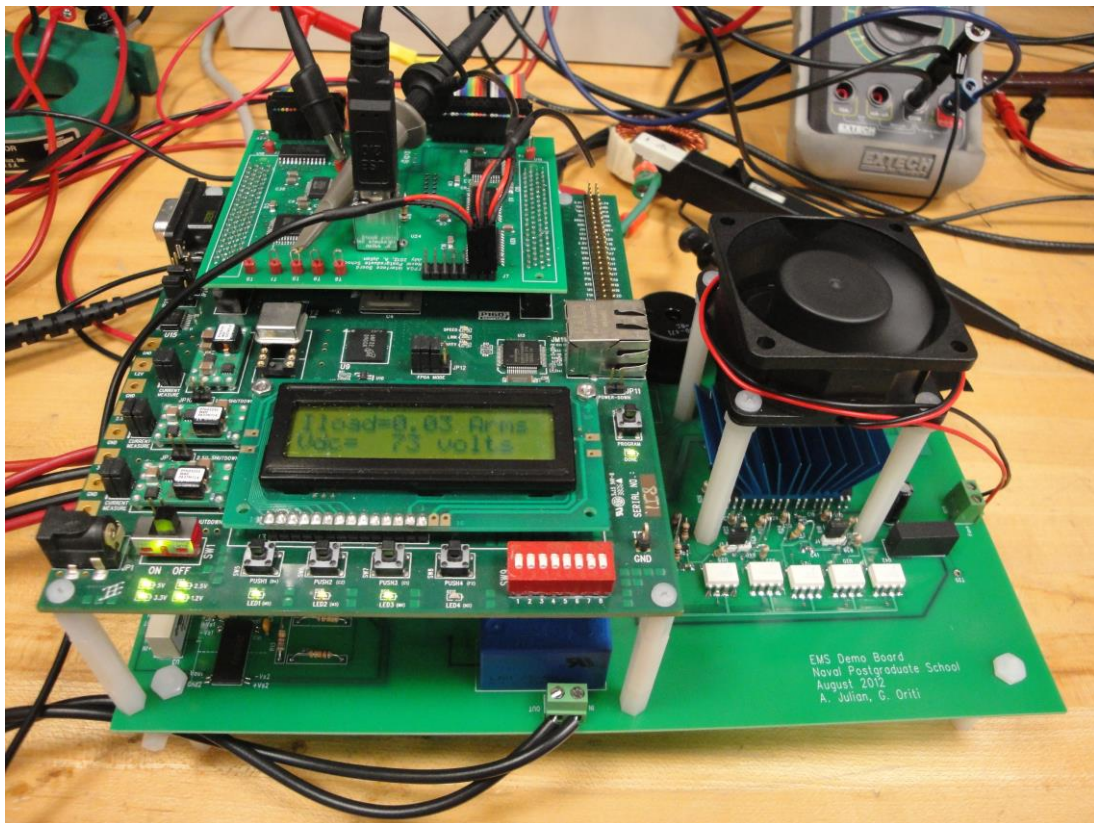
Figure 15.   EMS used in Laboratory to Collect CM and DM Voltages and
Currents. Source: [9].
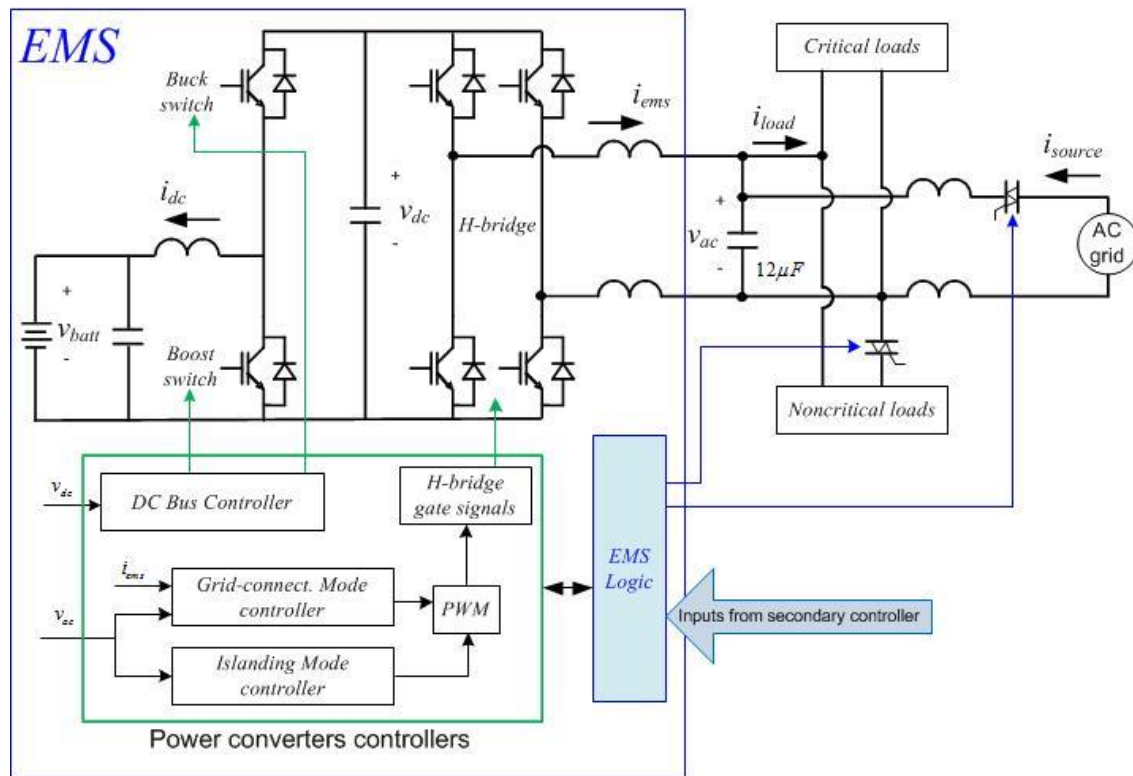
Figure 16. Circuit Diagram of EMS Used in Laboratory. Source: [9].

Table 3.   A List of Parameters Used for Simulink and Laboratory
Experiments.

Parameters	Simulink	Laboratory
$f_{switching}$	17.4 kHz	17.4 kHz
V_{DC}	200.0 V	200.0 V
V_{AC}	110.0 V (RMS)	110.0 V (RMS)
$R_{parasitic}$	2.0 Ω	unknown
L_1	247.0 μH	247.0 μH
L_2	247.0 μH	247.0 μH
L_m	25.0 μH	25.0 μH
$L_1 + L_2$	950.0 μH	950.0 μH
C	12.0 μF	12.0 μF
R_{Load}	133.33 Ω	133.33 Ω
L_{Load}	0.1846 H	0.1846 H
$C_{parasitic}$	10.0 nF	unknown
L_{Boost}	300.0 μH	300.0 μH
C_{Boost}	1320.0 μF	1320.0 μF

C.   COMPARISON OF RESULTS

Using both unipolar and bipolar PWM, three measurements were taken in the laboratory, the DM current I_{ems}, CM current I_{cm} and DM load voltage V_{ac}, all shown in Figure 9. Using these three measurements, we compared the laboratory and Simulink results. MATLAB was used to interpret and plot the data; the code is included in the Appendix. The Appendix shows that the laboratory data was imported from Excel while omitting the first 15 points. These cells contained header data not relevant to the actual measurements.

The load voltages shown in Figure 17 and Figure 18 allow a comparison of the laboratory and Simulink results for bipolar and unipolar PWM, respectively. The horizontal axis is time in seconds and the vertical axis is the voltage in volts. Both simulated and experimental voltages have a peak of approximately 150.0 V, or approximately 110.0 V root-mean squared (RMS). One major difference between the laboratory waveforms and the Simulink waveforms is that there is more noise in the laboratory results. The noise is prevalent in lower harmonics from 100.0 Hz to 1.0 kHz. This noise does not show up in the simulated waveforms because ideal switches and sources were used in the Simulink model.

It is widely understood that voltage harmonics exist in the grid due to non-linear loads [10]. Using the fast Fourier transform (FFT) in MATLAB, we plotted the frequency spectrum compared to voltage. The comparison of the Simulink and laboratory results is shown in Figure 19 and Figure 20, respectively. Primarily, the fifth and seventh harmonics are prevalent in the laboratory results, shown in red, but are not present in the spectral analysis of the Simulink model results, which is represented in blue.

Further information concerning harmonic distortion on the grid can be found in [10]. The presence of the fifth and seventh harmonics is to be expected when in grid-connected mode [10]. To refine the Simulink model one can inject these harmonics into the simulation. We can forgo this addition, as it is widely understood that these harmonics are present, and the addition of these harmonics would ultimately have minimal effect on the rest of this thesis.
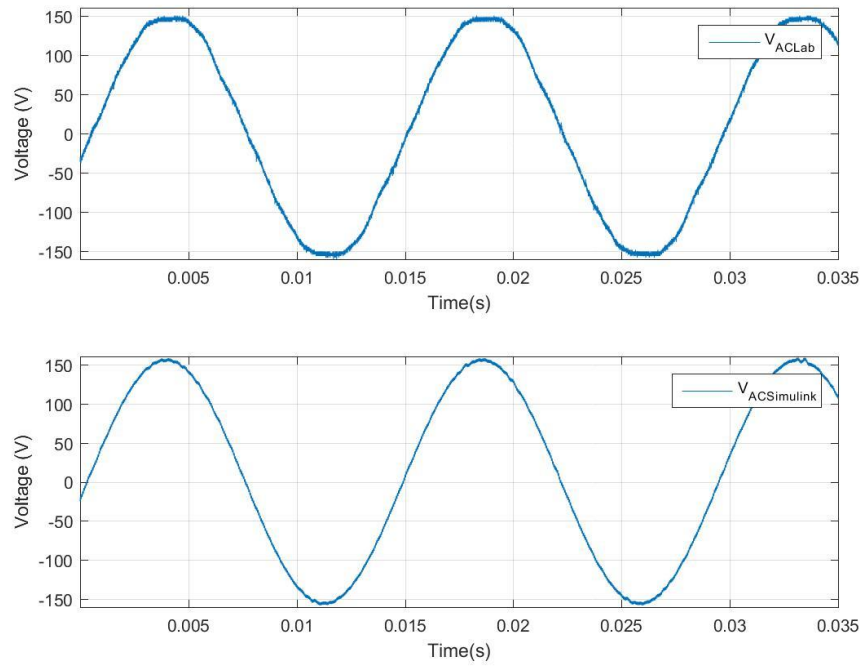
19

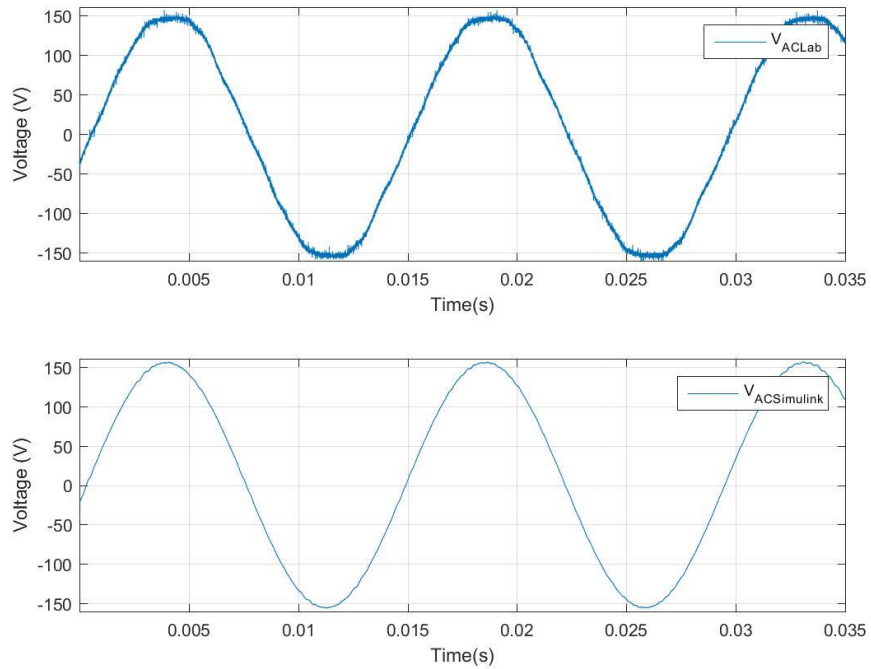Figure 17.   AC Load Voltage Waveforms for Laboratory and Simulink Using Bipolar PWM.

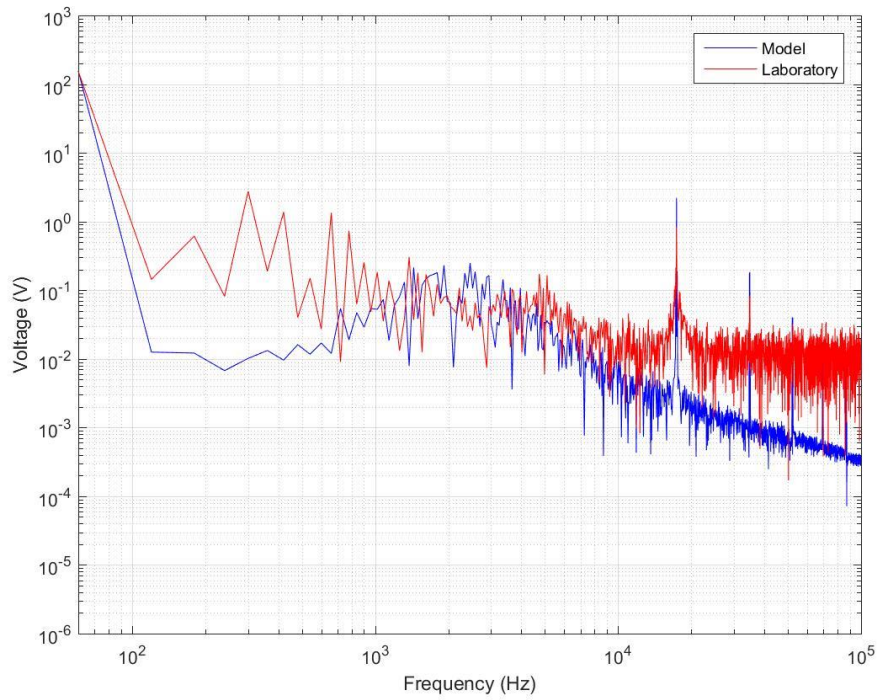Figure 18.   AC Load Voltage Waveforms for Laboratory and Simulink Using Unipolar PWM.

20

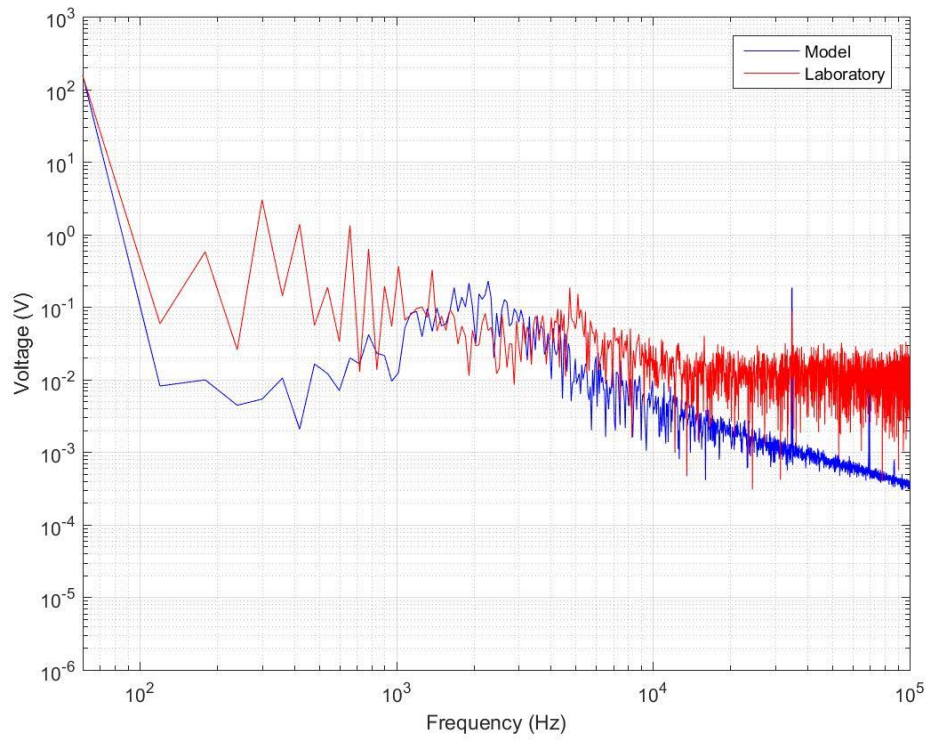Figure 19.   Spectral Analysis for DM Voltage using Bipolar PWM.

Figure 20.   Spectral Analysis for DM Voltage using Unipolar PWM.

21

1. Comparison of Results for Bipolar PWM

Using bipolar PWM, we can expect little to no CM current; however, the DM current is much larger than the DM current for unipolar PWM. Shown in Figure 21 is the DM current for both the laboratory and Simulink model. The horizontal axis is time in seconds and the vertical axis is current in amperes. The DM current for the Simulink model varies from the laboratory prototype due to model simplifications. For the Simulink model, we used ideal switches, and in the prototype, we used IGBT's; however, the amplitude and phase of the waveform are similar to that obtained for the laboratory model results.
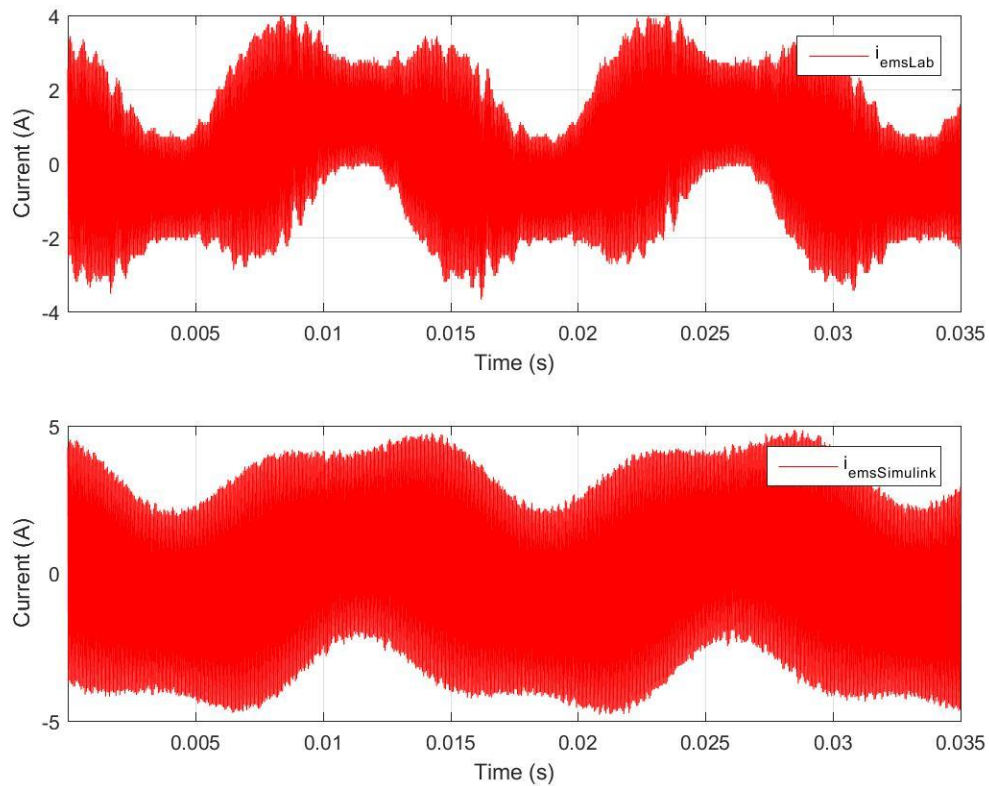

Figure 21. EMS Current for Laboratory and Simulink Using Bipolar PWM.

As predicted and shown in Figure 22, the CM current is essentially zero for bipolar PWM. The top plot represents the CM current in the laboratory, while the bottom plot is representative of the CM current in the Simulink model. The difference in the plots

may be caused by higher order affects not taken into consideration in this thesis. Also, as previously stated, ideal switches were used, which can also account for some of the error between the two plots. This Simulink model is able to predict the results accurately and can be used for further analysis of the EMS.
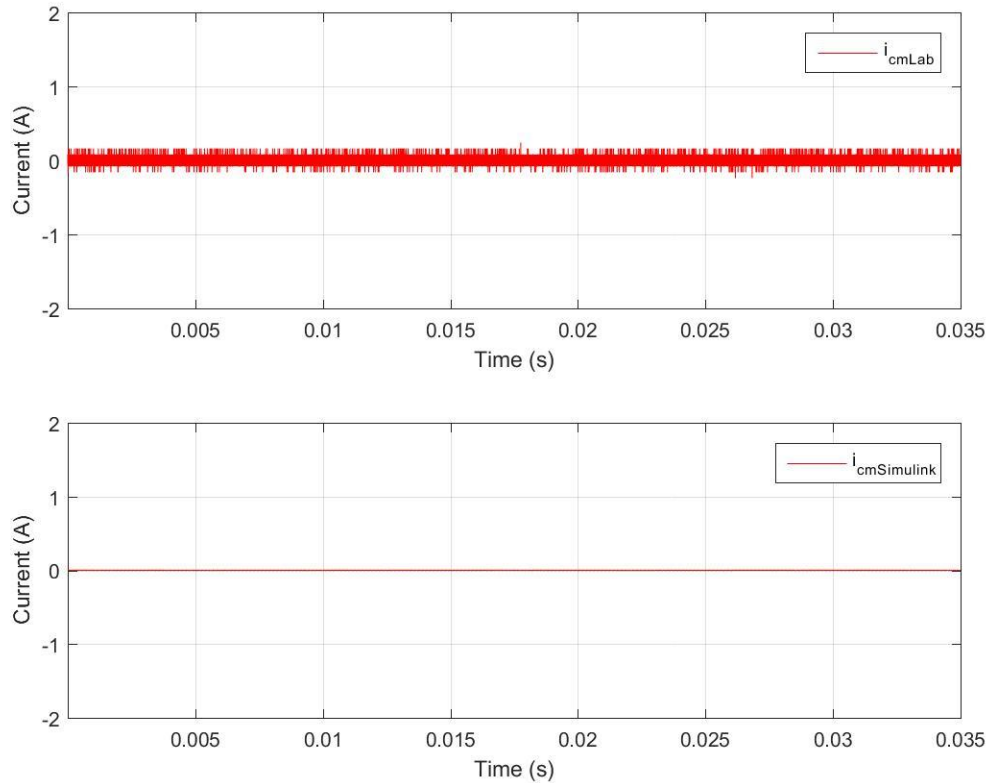
Figure 22.   CM Current for Laboratory and Simulink Using Bipolar PWM.

2.   Comparison of Results for Unipolar PWM

For the second part of the laboratory experiment, we used unipolar PWM. The DM and CM currents are plotted in Figure 23 and Figure 24, respectively. In both figures, time is in seconds for the horizontal axis and current in amperes for the vertical axis. The laboratory and Simulink waveforms for both the DM and CM currents are almost exact replicas of each other. Looking closely at Figure 23 and Figure 24 allows us to determine that there are slight differences between the model and the laboratory waveforms.   The higher order effects and the modeling difference discussed previously account for these

differences. Overall, this model is able to predict the results accurately; therefore, it can be used for further analysis.
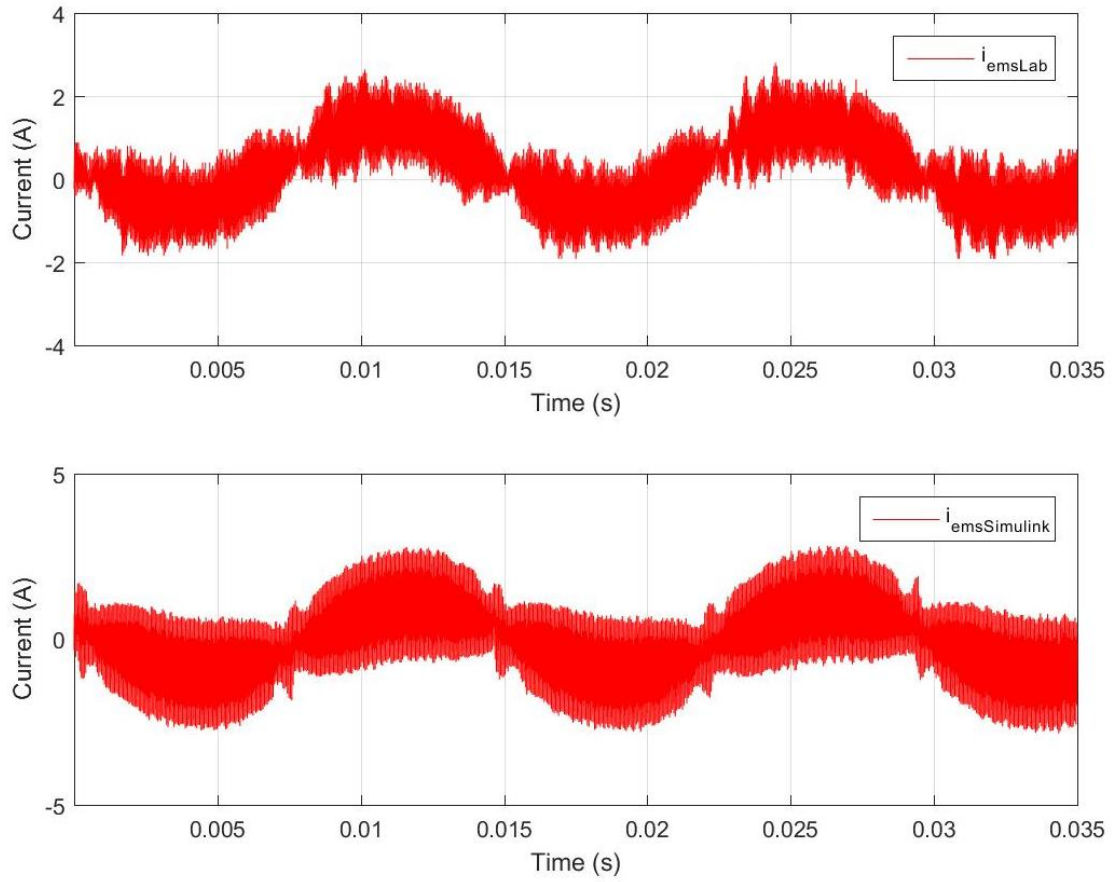
Figure 23.   EMS Current for Laboratory and Simulink Using Unipolar PWM.
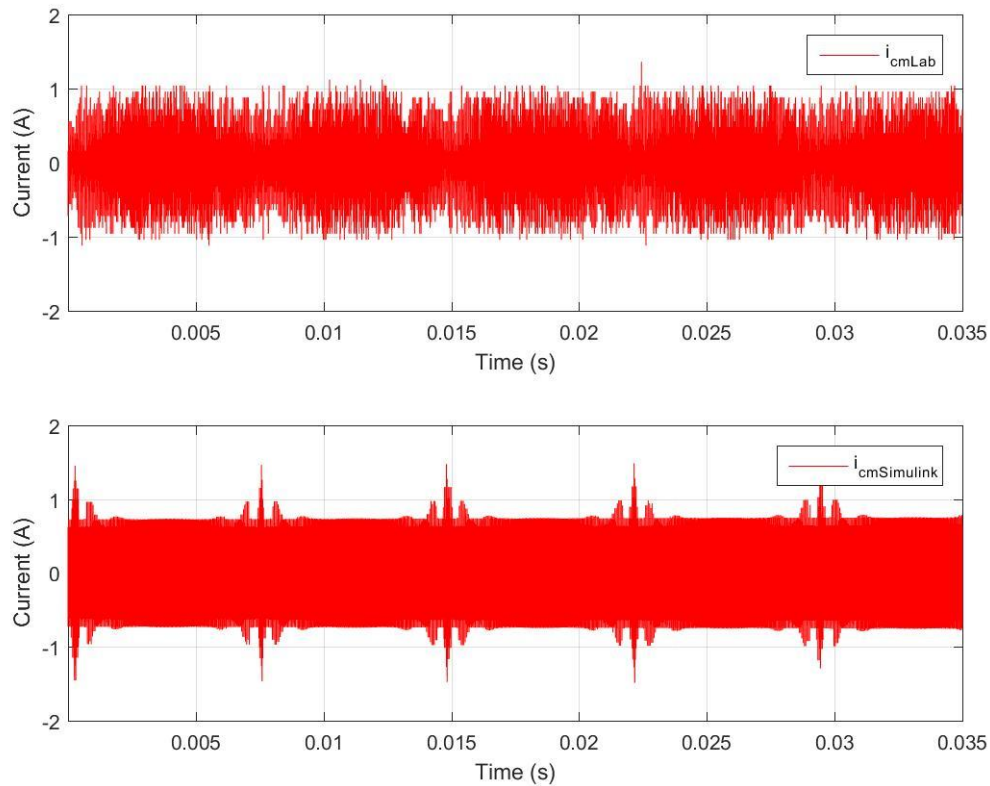
Figure 24.   CM Current for Laboratory and Simulink Using Unipolar PWM.

3.   LISN Voltage and Need for Additional Filters

Both unipolar and bipolar PWM are common methods used to control power electronics. When determining which method to use it is important to understand the design requirements. For the purpose of this thesis, we use MIL-STD 461 CE102. This standard sets the voltage limit level in dBμV across a frequency spectrum of 10 kHz to 10 MHz. This limit is plotted in red for Figure 25 and Figure 26. In order to measure the voltage, we needed a LISN. The measurements from the LISN go through a 20-dB attenuator. Once this data is collected, it has to be converted from voltage to dBμV. Given the dBμV data, the FFT function in MATLAB was used to obtain and plot the results. The blue plots shown in Figure 25 and Figure 26 represent the LISN voltage for bipolar and unipolar PWM, respectively.

25
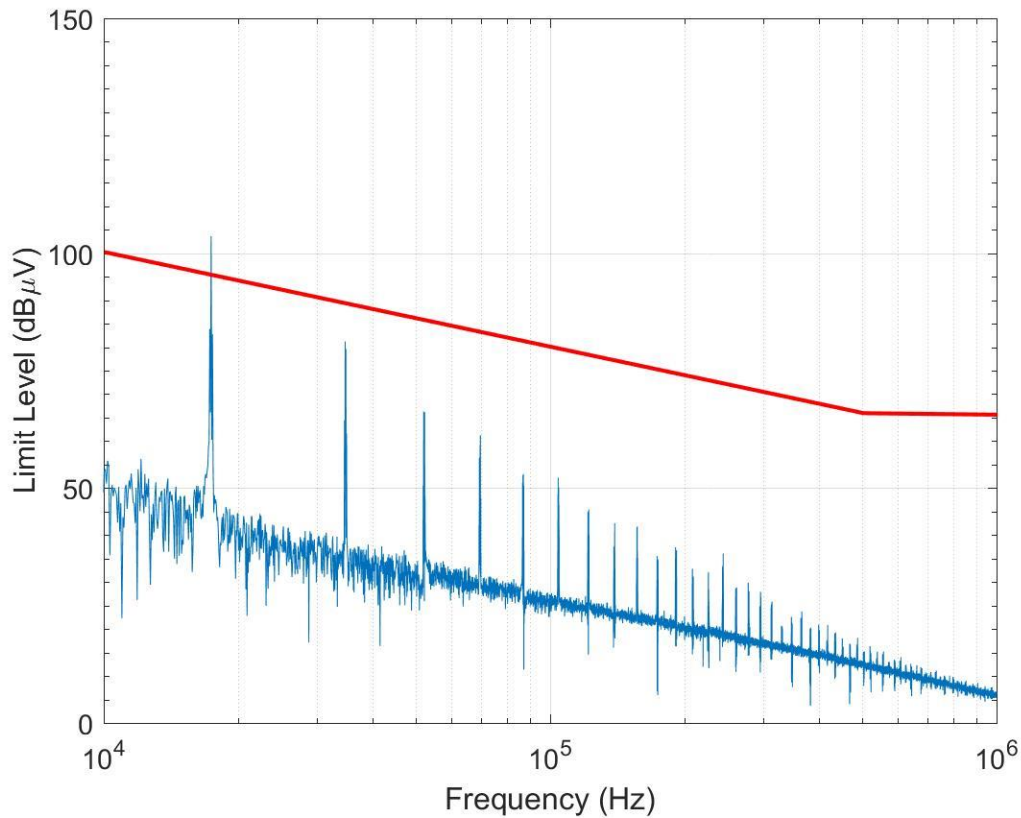
Figure 25.   LISN Voltage Compared to MIL-STD 461 Using Bipolar PWM.

The data plotted in Figure 25 represents the LISN voltage compared to the MIL-STD for bipolar PWM. Using this modulation strategy is advantageous when compared to the MIL-STD. For most of the frequency spectrum, the LISN voltage is below the limit level; however, it appears that at approximately 1800 kHz, the limit level is not within standards. The addition of a DM filter should reduce the DM voltage and current and bring the LISN voltage within the MIL-STD limit level. When designing a DM filter, one must consider the size of the inductor. Generally, space is a premium onboard a naval vessel; therefore, adding an appropriately sized inductor saves space and money.
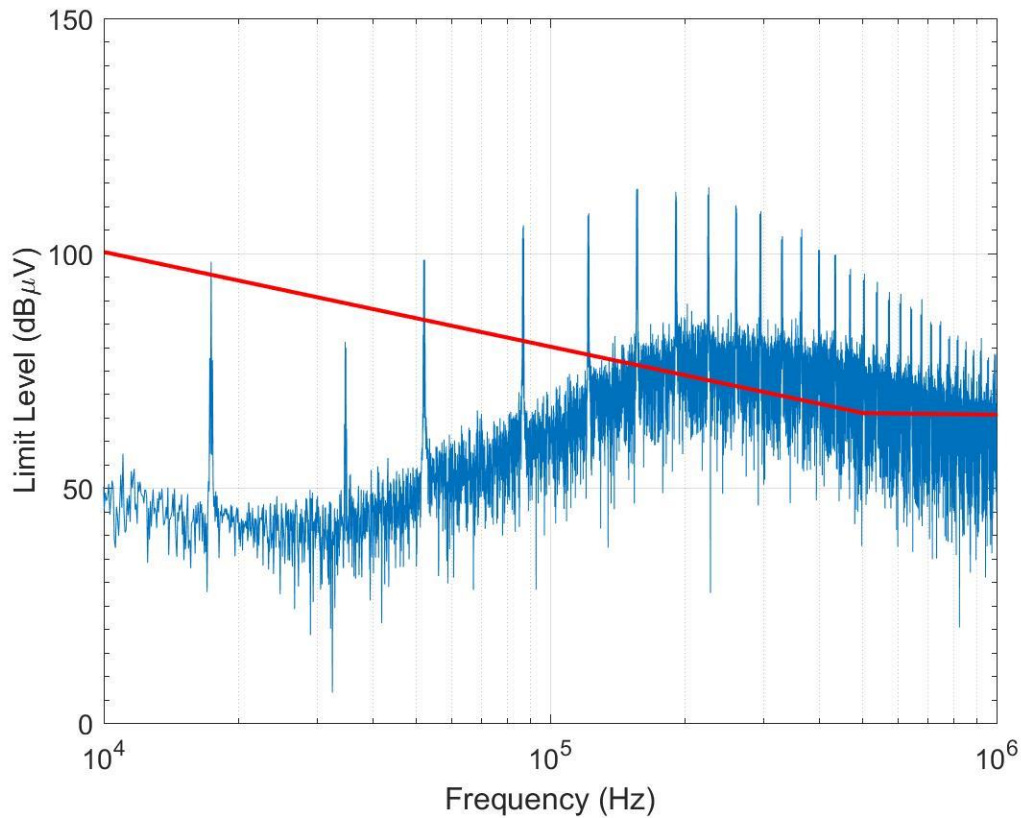
Figure 26.   LISN Voltage Compared to MIL-STD 461 Using Unipolar PWM.

Using unipolar PWM to gate the IGBTs produces an unwanted CM current as shown in Figure 26. This leakage current causes this design to be out of standard when compared to the MIL-STD. Across the entire frequency spectrum, we note that the LISN voltage is drastically out of standards. Based on Figure 25 and Figure 26, we assume that bipolar PWM requires less filtering in order to be within standard.

Implementing a CM choke to reduce the leakage current will bring this design within the prescribed limit levels. Generally, CM chokes are very large and expensive. Since budget and space are always a concern onboard a naval vessel, this is definitely something that must be taken into consideration.

THIS PAGE INTENTIONALLY LEFT BLANK

IV. UPDATED MODEL WITH FILTER DESIGN

As stated in the previous chapter, both modulation strategies require filtering to meet the conducted EMI limits set by MIL-STD 461. The design of these filters varies for both unipolar and bipolar PWM. When using unipolar PWM, the conducted EMI is in the CM path. CM noise is a voltage or current measured between power lines and ground [11]. When designing a filter to eliminate the conducted EMI for the CM path, we must consider the current and voltage paths to ground. For bipolar PWM, the conducted EMI is in the DM path. DM noise is in the line-to-line voltages and currents [11]. From this, we see that we must design different filters for each modulation strategy. These filters will vary in size and cost, and based on the end users' design requirements and budget, we can determine which modulation strategy is most effective.

A.   DIFFERENTIAL FILTER

Generally, DM filters require an inductor in the current path to eliminate conducted EMI. The circuit shown in Figure 27 is the circuit diagram used to for bipolar PWM. When compared to Figure 9, which is the circuit diagram without the DM filter, we note the addition of two inductors L on the top and bottom legs of the inverter. These inductors each have a value of 1.25 mH. To implement this in Simulink, we used the inductor block from the SimPowerSystems library.

The addition of the DM filter performed as expected. The DM current i_{ems} from the initial laboratory simulations and the filtered Simulink results are shown in Figure 28. On the horizontal axis, time is in seconds, while the current is in amperes on the vertical axis. The filtered results in Figure 28 show how the addition of an inductor on both the top and bottom legs on the inverter can drastically reduce the conducted EMI in the system. A larger inductor filters out more of the noise; however, we must also consider the overall design of the circuit. It was the intent to design a filter that ensured that the single-phase grid tied inverter met the requirements of MIL-STD 461 while minimizing the size of the filter.
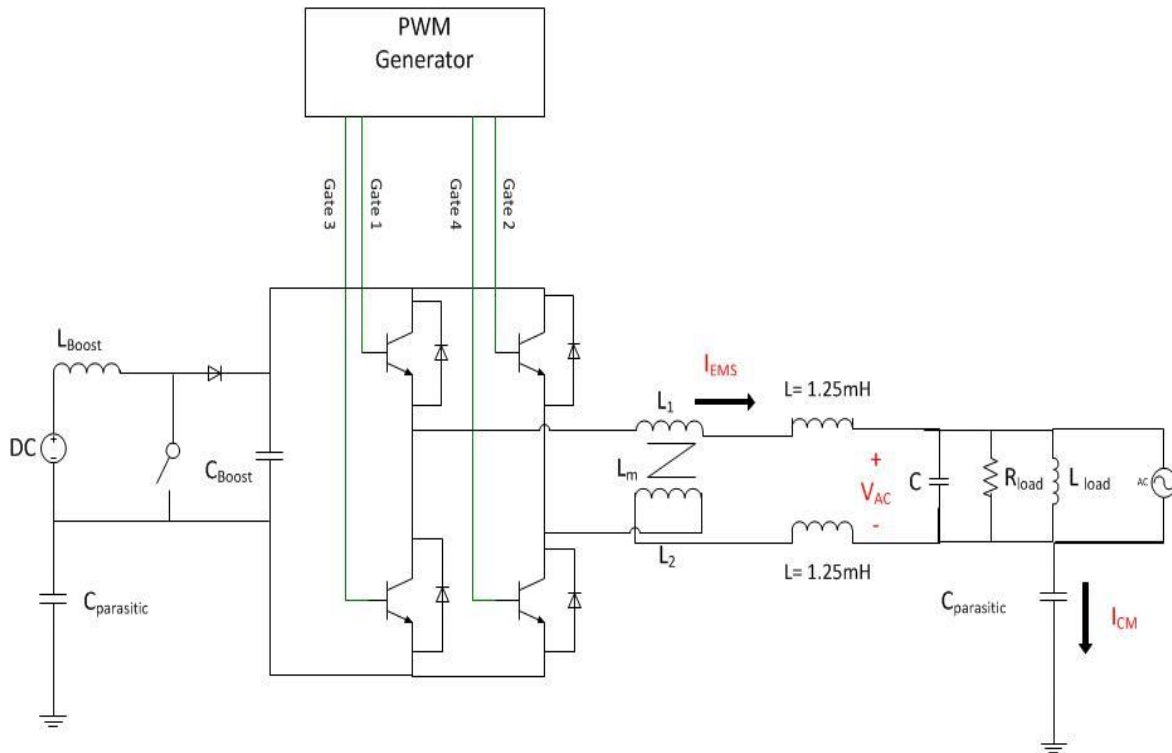
Figure 27.   Circuit Diagram with DM Filter for Bipolar PWM
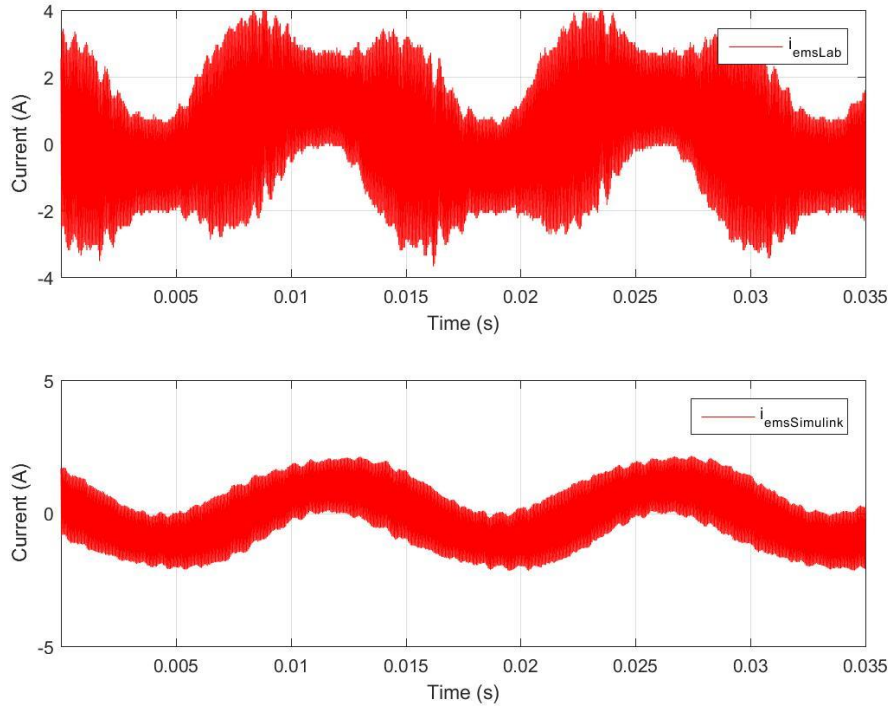
Figure 28.   EMS Current for Laboratory and Filtered Simulink Model using
Bipolar PWM

When comparing the laboratory results to the filtered results of the Simulink model, as shown in Figure 28, it is apparent that the conducted EMI is drastically reduced. Next, we consider the LISN voltage with respect to MIL-STD 461. As shown in Figure 29, the LISN voltage is below the MIL-STD; therefore, we conclude that the addition of a simple filter reduces the conducted EMI and brings it within design requirements. In general, MIL-STD 461 applies from 10.0 kHz to 10.0 MHz; however, we only examined the spectrum to 1.0 MHz. Due to the model simplifications stated in Chapter III, we do not believe this model accurately predicts the behavior past the 1.0-MHz range.

Figure 29.   LISN Voltage of Filtered Simulink Model Compared to MIL-STD 461 Using Bipolar PWM

B.   COMMON MODE CHOKE

Many designs exist for CM noise suppression. In this thesis, we used a common-mode choke, which is a magnetically coupled set of inductors. These inductors share a

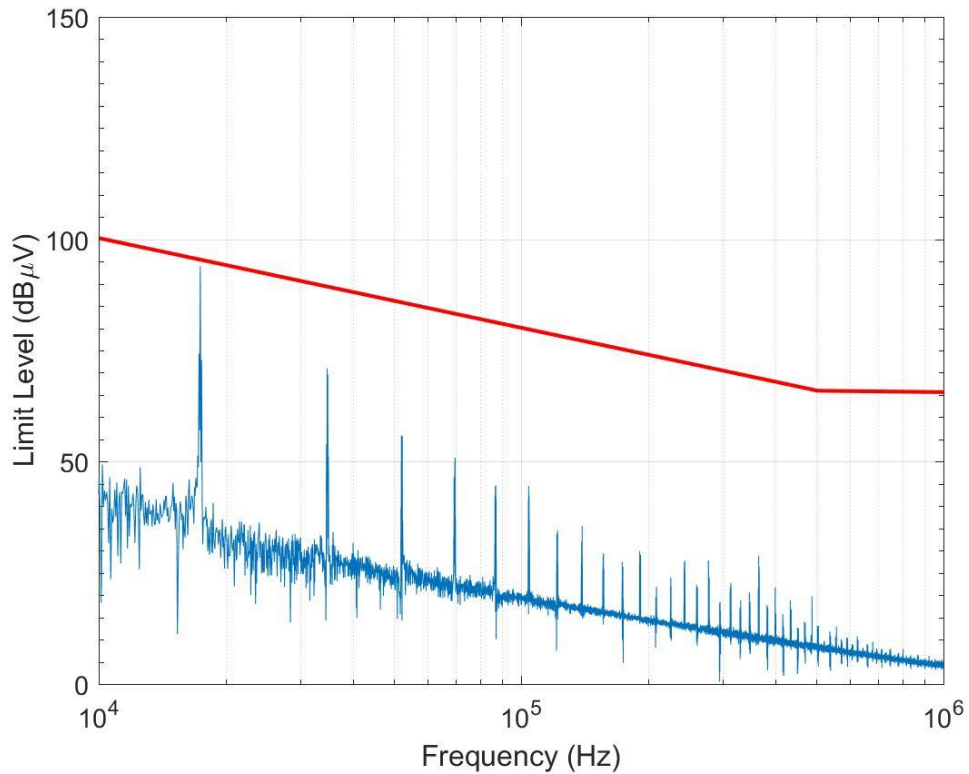common core, which essentially eliminates the CM conducted EMI. To implement this in the Simulink model, we first set the PWM generator to unipolar PWM and then insert a mutual inductance block from the SimPowerSystems library to simulate a CM choke. The mutual inductance block is comprised of the leakage inductance L_{l1} and L_{l2}, and the magnetizing inductance L_{m1} and L_{m2}. The inductance matrix

$$\begin{pmatrix} L_{l1} + L_{m1} & \dfrac{N_1}{N_2} L_{m1} \\ \dfrac{N_1}{N_2} L_{m2} & L_{l2} + L_{m2} \end{pmatrix} \tag{7}$$

shows that both L_{m1} and L_{m2} are multiplied by N_1/N_2, which is known as the turns ratio. In this design, the turns ratio is one. The inductance matrix

$$\begin{pmatrix} 50.0\ \mu H + 50.0\ mH & 50.0\ mH \\ 50.0\ mH & 50.0\ \mu H + 50.0\ mH \end{pmatrix} \tag{8}$$

was the input for the Simulink mutual inductance block. Shown in Figure 30 is the circuit diagram used. It is the same circuit shown in Figure 9 with the addition of a CM choke.
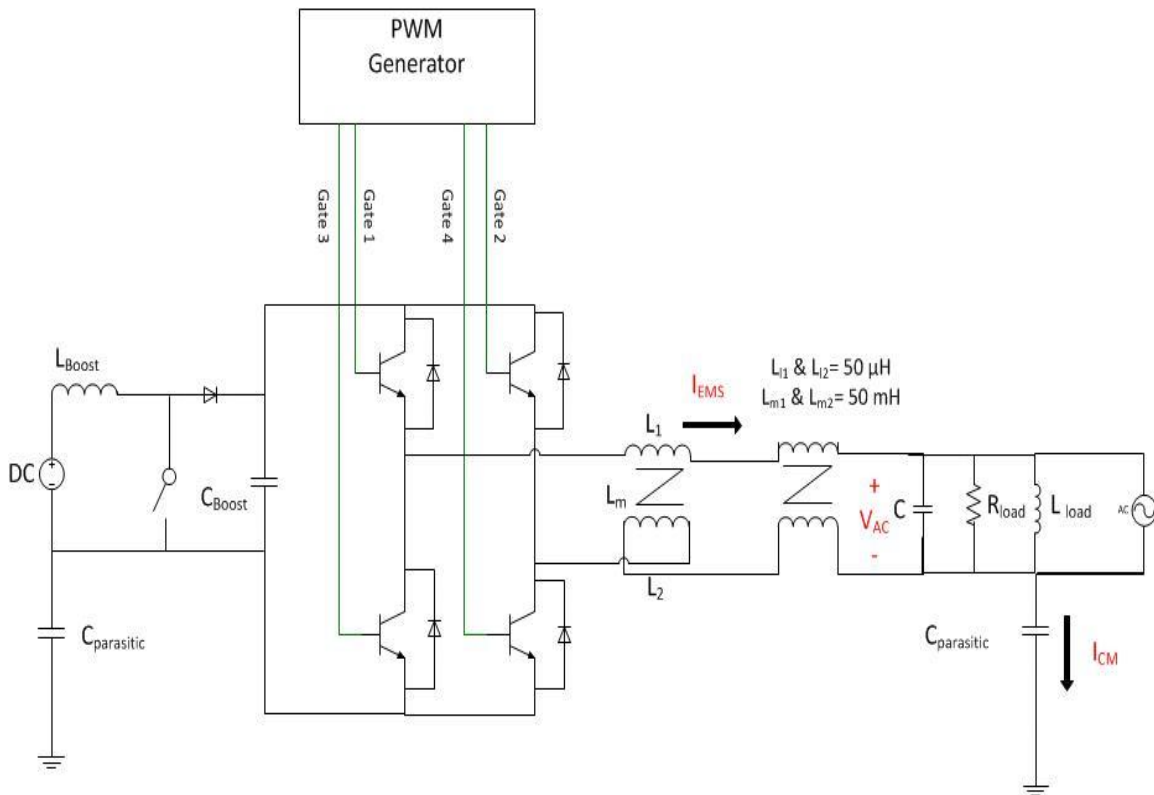
Figure 30.   Circuit Diagram with Common Mode Choke for Unipolar PWM.

The addition of a CM choke reduces the conducted EMI. The CM current from the initial laboratory measurements and the filtered Simulink results are shown in Figure 31. The horizontal axis is time in seconds, and the vertical axis is current in amperes. Using a CM choke to eliminate the CM current for a single-phase grid tied inverter is a viable filtering technique.

The next step is to see if the filter reduced the conducted emissions enough to meet MIL-STD 461. In order to check this, we used the LISN voltage as described in Chapter III and performed an FFT. This analysis was performed in MATLAB. Shown in Figure 32 is the comparison between the MIL-STD and the LISN voltage. The LISN voltage is below the MIL-STD. From this, we conclude that a simple CM choke eliminates the CM conducted emissions.

Figure 31.   CM Current for Laboratory and Filtered Simulink Model Using Unipolar PWM

Figure 32.   LISN Voltage of Filtered Simulink Model Compared to MIL-STD 461 Using Unipolar PWM

V.   CONCLUSION

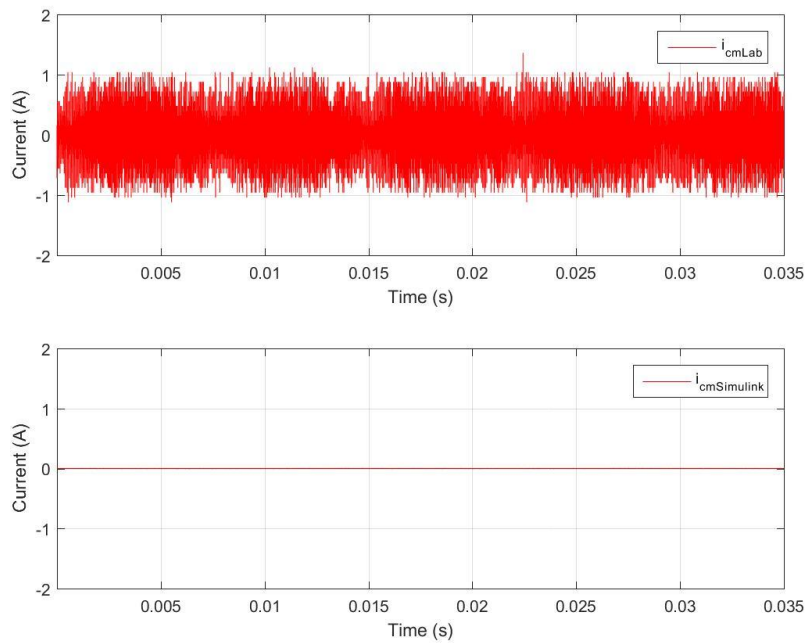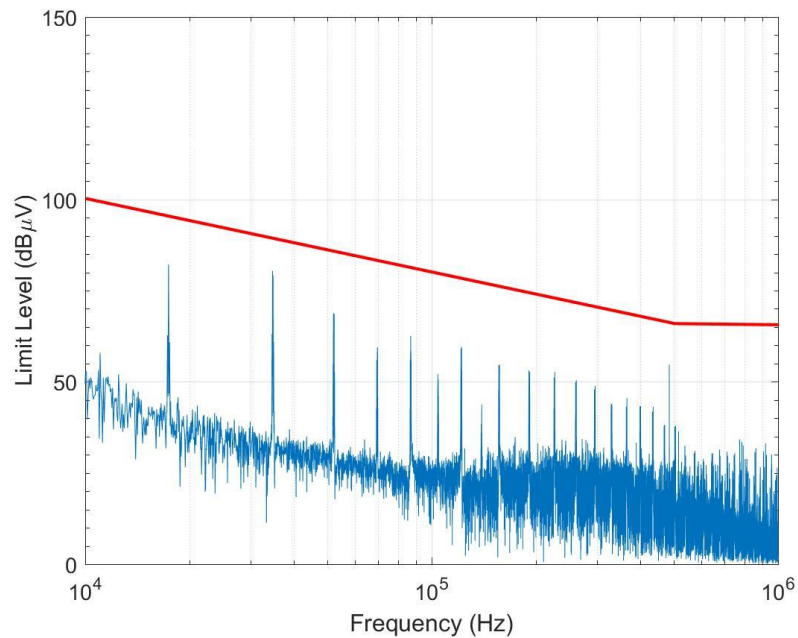Both unipolar and bipolar PWM create conducted EMI. This unwanted noise appears in both the differential and common mode paths of the circuit. These emissions can cause faults or failures on the grid if not controlled. In this thesis, MIL-STD 461 CE102 was used as a design metric. Using this standard, we designed our differential and common mode filters to meet this requirement.

In order to accomplish the aforementioned, we first designed a Simulink model of a single-phase grid-tied inverter. Using this model and the EMS designed in the laboratory, we were able to compare the CM and DM currents. Based on the measurements taken, we concluded that the Simulink model accurately represented the laboratory model with a few exceptions, which were clarified in Chapter III. The model was next refined by adding a LISN to measure the AC voltage for the EUT. This voltage was converted to *dBμV* and then a spectrum analysis from 1.0 KHz to 1.0 MHz was performed. Based on these results, it was determined that a differential and common mode filter must be added to meet the MIL-STD.

For the DM filter, we added an inductor to the top and bottom legs of the inverter. For the CM filter, we used a mutual inductor. Both of these filters ultimately met MIL-STD 461. Using passive filters to reduce conducted emissions in a single-phase grid tied inverter is a feasible way to meet the design standard.

Ultimately, the decision between using unipolar or bipolar PWM depends on the design parameters. Bipolar PWM has minimal CM currents and voltage while unipolar does not. Vice versa, unipolar PWM produces minimal DM currents and voltages while bipolar does not. Depending on design requirements, one may choose one modulation strategy over the other.

A.   FUTURE WORK

Based on the results of this thesis, it is pertinent to examine the filter design for both DM and CM filters in more detail. The next step is to look into the inductor design. In doing this, we can compare the size and displacement of the inductors and then

determine which modulation strategy is more cost effective. This allows the engineer to pick a modulation strategy that ultimately meets his desired cost, size and standard for a single-phase inverter. In addition, other topologies for the inverter should be explored.

APPENDIX

```matlab
%% Thesis Plots
% Jason Valiani: Single Phase Power Inverters
clc; close all
% %% Plots for PWM Generator
% figure(1)
% hold on
% plot(time,Vgate); xlabel('Time (s)'); ylabel('Voltage (V)');
% plot(time,Vdc.*sin(2*pi*60.*time),'r', 'linewidth',2);
% hold off


%% Data from Lab:
% Inport data from scope readings: add bipolar after wfm. to analyze
bipolar

% vacx=xlsread('Tek_CH1_Wfm.csv');
% i_emsx=xlsread('Tek_CH2_Wfm.csv');
% i_cmx=xlsread('Tek_CH4_Wfm.csv');
%
vacx=xlsread('Tek_CH1_Wfm_bipolar.csv');
i_emsx=xlsread('Tek_CH2_Wfm_bipolar.csv');
i_cmx=xlsread('Tek_CH4_Wfm_bipolar.csv');

% Adjust data, first 15 rows are other information
len = length(vacx);
timestep_L=3.5e-7;
time_vec_L=(0+timestep_L:timestep_L:.035);    %Time vector
vac_L=vacx(15:len,2);           %AC Voltage
i_ems_L=i_emsx(15:len,2);       %Differntial Mode Current
i_cm_L=i_cmx(15:len,2);         %Common Mode Current

% Adjust Lab data for FFT
one_cycle_L=round(1/60/4e-7) %4e-7 is sample time
vac_ss_L=vac_L(1:one_cycle_L);
iems_ss_L=i_ems_L(1:one_cycle_L);
icm_ss_L=i_cm_L(1:one_cycle_L);
vac_spect_L=fft(vac_ss_L)*2/one_cycle_L;

freq_L=[0:one_cycle_L-1]*60;
tmin_L=time_vec_L(1);
tmax_L=max(time_vec_L);

%% Simulink Data for Common and Differential Mode
timestep=3.5e-7;
time_vec=(0:timestep:.035);     %Time vector

% Adjust Simulink Data for FFT
one_cycle=round(1/60/4e-7) %4e-7 is sample time
vac_ss=Vac(15*one_cycle:15*one_cycle+one_cycle);
vs_ss=vs(15*one_cycle:15*one_cycle+one_cycle);
```

```matlab
vac_LISN_ss=Vac_LISN(15*one_cycle:15*one_cycle+one_cycle);

vac_spect=fft(vac_ss)*2/one_cycle;
vs_spect=fft(vs_ss)*2/one_cycle;
vac_LISN_spect=fft(vac_LISN_ss)*2/one_cycle; %micro volts

freq=[0:one_cycle]*60;
tmin=time_vec(1);
tmax=max(time_vec);

%% Plot of AC Voltoage
figure(2)
% Lab
ax1=subplot(2,1,1);
plot(time_vec_L,vac_L)
xlabel('Time(S)')
ylabel('Voltage (V)')
grid on
axis([tmin_L tmax_L -160 160])
legend('V_A_C_L_a_b')

% Simulink
ax2=subplot(2,1,2);
plot(time_vec,Vac(15*one_cycle-1000:(15*one_cycle-1000)+100000,1))
xlabel('Time(S)')
ylabel('Voltage (V)')
grid on
legend('V_A_C_S_i_m_u_l_i_n_k')
axis([tmin tmax -160 160])
linkaxes([ax1,ax2],'x');
saveas(gcf,'Bipolar_SM_Lab_Vac','jpeg');
%% Lab and Simulink Results for  I_EMS
figure(3);
% Lab
ax3=subplot(2,1,1);
plot(time_vec_L, i_ems_L,'r');
xlabel('Time (S)');
ylabel('Current (A)');
grid on;
axis([tmin_L tmax_L -4 4])
legend('i_e_m_s_L_a_b','Location','Northeast');
% Simulink
ax4=subplot(2,1,2);
plot(time_vec,Iac(15*one_cycle+20000:(15*one_cycle+20000)+100000,1),'r'
);
xlabel('Time (S)');
ylabel('Current (A)');
grid on;
legend('i_e_m_s_S_i_m_u_l_i_n_k','Location','Northeast');
axis([tmin tmax -5 5])
linkaxes([ax3,ax4],'x');
saveas(gcf,'Bipolar_SM_Lab_Iems','jpeg');
%% Lab and Simulink Results for  I_CM
figure(4)
% Lab
```

```matlab
ax5=subplot(2,1,1);
plot(time_vec_L, i_cm_L,'r');
xlabel('Time (S)');
ylabel('Current (A)');
grid on
axis([tmin_L tmax_L -2 2])
legend('i_c_m_L_a_b','Location','Northeast');

% Simulink
ax6=subplot(2,1,2);
plot(time_vec,Icm(15*one_cycle+20000:(15*one_cycle+20000)+100000,1),'r'
);
xlabel('Time (S)');
ylabel('Current (A)');
grid on
legend('i_c_m_S_i_m_u_l_i_n_k','Location','Northeast');
axis([tmin tmax -2 2])
linkaxes([ax5,ax6],'x');
saveas(gcf,'Bipolar_SM_Lab_Icm','jpeg');

%% Plot Harmonics in Log Log scale for AC voltage
figure(5)
loglog(freq,abs(vac_spect),'b',freq_L,abs(vac_spect_L),'r');
xlabel('Frequency (Hz)');
ylabel('Voltage (V)');
legend('Model','Laboratory ','Location','Northeast');
grid on;
axis([0 100000  10^-6 10^3]);
saveas(gcf,'Bipolar_SM_Lab_Harmonic','jpeg');

%% Plot LISN Voltage
figure(6)
semilogx(freq,abs((20*log10(vac_LISN_spect*10^6))));
xlabel('Frequency (Hz)');
ylabel('Limit Level (dB\muV)');
grid on
axis([10^4 10^7 0 150])
set(gca,'XMinorTick','on','YMinorTick','on')
set(gca,'fontsize',14)
% Create line for MIL-STD
annotation(figure(6),'line',[0.13125 0.57],...
    [0.653059040590406 0.468634686346863],'Color',[1 0
0],'LineWidth',3);
% Create line for MIL-STD
annotation(figure(6),'line',[0.56875 0.905625],...
    [0.468557195571956 0.467712177121771],'Color',[1 0
0],'LineWidth',3);
saveas(gcf,'Bipolar_SM_Lab_LISN','jpeg');
```

THIS PAGE INTENTIONALLY LEFT BLANK

LIST OF REFERENCES

[1]   Office of the Chief of Naval Operations. October 2010. "A Navy energy vision for the 21st Century" [Online]. Available: http://www.greenfleet.dodlive.mil/files/2010/10/Navy-Energy-Vision-2010.pdf. Accessed 28 March 2016.

[2]   M. H. Hedayati and J. Vinod, "Filter configuration and PWM method for single phase inverters with reduced conducted EMI noise," *IEEE Transactions on Industry Applications,* vol. 51, no. 4, pp. 3236–3243, Jan. 2015.

[3]   *DOD Interface Standard Requirments for the Control of Electromagnetic Interference Characteristics of Subsystems and Equipment*, MIL-STD-461 CE 102, 1999.

[4]   N. Mohan, T. M. Undeland, and W. P. Robbins, *Power Electronics. Converters, Applications, and Design,* 3rd ed., Hoboken, NJ: John Wiley & Sons, pp. 211–218, 2003.

[5]   A. Namboodiri and H. S. Wani, "Unipolar and bipolar PWM inverter," *International Journal for Innovative Research in Science & Technology*," vol. 1, no. 7, pp. 237–243, Dec. 2014.

[6]   J. W. Nilsson and S. A. Riedel, "Introduction to frequency selective circuits," in *Electric Circuits*, Upper Saddle River, NJ: Pearson Prentice Hall, pp. 522–550, 2011.

[7]   P. R. Clayton, *Introduction To Electromagnetic Compatibility*, Hoboken, NJ: John Wiley & Sons, pp. 25–26, 2006.

[8]   A. Consoli, G. Oriti, A. Testa, and A. L. Julian, "Induction motor modeling for common mode and differential mode emission evaluation," presented at Industry Applications Conference Thirty-First IAS Annual Meeting, San Diego, CA, 1996.

[9]   G. Oriti, A. L. Julian and N. J. Peck, "Power-electronic-based energy management system with storage," *IEEE Transactions on Power Electronics,* vol. 31, no. 1, pp. 452–460, Jan 2016.

[10] S. J. Pierce, "Reducing stator current harmonics for a doubly-fed induction generator connected to a distorted grid," M.S. thesis, Electrical Engineering, Naval Postgraduate School, Monterey, Sep 2013.

[11] N. Mohan, T. M. Undeland and W. P. Robbins, *Power Electronics Converters, Applications, and Design*, 3rd ed., Hoboken, NJ: John Wiley & Sons, pp. 500–502, 2003.

INITIAL DISTRIBUTION LIST

1.   Defense Technical Information Center
      Ft. Belvoir, Virginia

2.   Dudley Knox Library
      Naval Postgraduate School
      Monterey, California